

國立交通大學

電信工程學系

碩士論文

應用於高速移動正交分頻多工系統分組子載波干擾
消除及資料偵測之研究

A Study on
Group Based ICI Cancellation and Data Detection for
High Mobility OFDM Systems

研究生：邱麟凱

指導教授：黃家齊 博士

中華民國九十六年六月

應用於高速移動正交分頻多工系統群組化子載波干
擾消除及資料偵測之研究

A Study on
Group Based ICI Cancellation and Data Detection for
High Mobility OFDM Systems

研究生：邱麟凱

Student : Li-Kai Chiu

指導教授：黃家齊

Advisor : Dr. Chia-Chi Huang

國立交通大學

電信工程學系碩士班

碩士論文

A Thesis

Submitted to Department of Communication Engineering

College of Electrical and Computer Engineering

National Chiao Tung University

in Partial Fulfillment of the Requirements

for the Degree of

Master of Science

in

Communication Engineering

July 2007

Hsinchu, Taiwan, Republic of China

中華民國九十六年七月

應用於高速移動正交分頻多工系統分組子載波干擾 消除及資料偵測之研究

學生：邱麟凱

指導教授：黃家齊

國立交通大學電信工程學系 碩士班



由移動所造成的頻道變化會使得一個正交分頻多工系統的符元有頻率選擇性的衰減，這樣的現象使傳統一級等化器的方法不能被利用，且此現象更進一步的會破壞子載波之間的正交性使得正交分頻多工系統的符元遭受到內部子載波互相干擾的現象，若是在高速移動的情況下會造成系統效能嚴重的被降低，為了減輕此現象帶來的問題，這篇文章提出一個運用球形解碼或列表式球形解碼反覆式的分組子載波干擾消除方法，在接收端子載波會被分成許多組，並使用球形解碼或列表式球形解碼去產生資訊再將這些資訊傳送到其它組做子載波干擾消除，分組的方法是用來減輕使用球形解碼或列表式球形解碼的計算複雜度，而子載波干擾消除的方法是用來使系統效能更好。

A Study on Group Based ICI Cancellation and Data Detection for High Mobility OFDM Systems

Student : Li-Kai Chiu

Advisor : Dr. Chia-Chi Huang

Department of Communication Engineering
National Chiao Tung University

ABSTRACT

The channel variation due to vehicle mobility produces frequency selective fading among OFDM symbols which makes the traditional one-tap equalizer can not be utilized. Moreover, the orthogonal property of OFDM subcarriers is destroyed and OFDM symbol experiences inter-carrier interference (ICI) that severely degrades the performance in high vehicle mobility environment. To reduce the problem, an iterative group based ICI cancellation method which applies sphere decoding and list sphere decoding (LSD) is proposed. At the receiver, subcarriers are partitioned into several groups, each group uses SD or LSD to generate the message information and pass it to other groups for ICI cancellation. The grouping procedure is used to reduce the computation complexity of the SD and LSD, and ICI cancellation procedure is used to make BER performance better.

誌謝

感謝黃家齊教授這兩年的教導，碩士論文上提供許多的建議和概念使得這一篇論文的完成更加的順利與完整，並且使我在這一段時間內對通訊領域有更進一步的了解。

這一篇論文的完成要特別感謝早安學長古孟霖，學長這兩年來不辭辛苦的解答我的問題與疑惑，並指導我論文的方向和細節以及可能需要注意的問題，更重要的讓我了解此研究在通訊領域上的相關問題和應用。

感謝這兩年一同患難的實驗室同學鄒鎧駿、吳其珍、杜欣憶，在研究及課業之餘，大家能以輕鬆談諧的談話使我將生活上壓力拋開。

最後感謝在我求學路程上不斷的支持的父母及家人。

Contents

中文摘要	i
ABSTRACT	ii
誌謝	iii
Contents	iv
List of Tables	vi
List of Figures	vii
Chapter 1 Introduction	1
Chapter 2 OFDM System in High Mobility Environment and Sphere Decoding	4
2.1 High Mobility Environment.....	4
2.2 ICI on OFDM System.....	6
2.3 Sphere Decoding.....	10
2.3.1 Real Sphere Decoding	10
2.3.2 Complex Sphere Decoding	17
2.4 List Sphere Decoding.....	21
Chapter 3 Grouped Based ICI Cancellation Method	24
3.1 System Model	24
3.2 Group based ICI Cancellation Method with Sphere Decoding.....	25
3.3 Group based ICI Cancellation Method with List Sphere Decoding	28
3.3.1... Soft Symbol	28
3.3.2 Conditional Probability.....	30
3.4 Radius of the Sphere	33
Chapter 4 Simulation Result	35



4.1	Simulation Environment	35
4.2	Simulation Result Discussions.....	38
4.2.1	Simulation in Environment I.....	38
4.2.2	Simulation in Environment II	50
4.3	Computational Complexity	58
Chapter 5 Conclusions		60
Bibliography		61



List of Tables

Table 4.1 Simulation parameters of the first kind of simulation environment.....36

Table 4.2 Simulation parameters of the second kind of channel simulation environment.....37

Table 4.3 Brief computational complexity comparison.....59

Table 4.4 Comparison of computational complexity under the second kind of channel.....59



List of Figures

Fig. 2.1 Base-band OFDM System.....	6
Fig. 2.2 A sphere of radius r and centered at $\mathbf{A}\hat{\mathbf{X}}$	13
Fig. 2.3 Sample tree generated to determine points in a N-dimensional sphere.	16
Fig. 2.4 Searching disk in 16-QAM.	18
Fig. 2.5 Sphere of SD or LSD in received signal domain.	22
Fig. 3.1 Group Method for ICI with window length $Q=2q+1$	26
Fig. 3.2 Block diagram of group based ICI cancellation method with Sphere Decoding.	28
Fig. 3.3 Block diagram of group based ICI cancellation with List Sphere Decoding.....	32
Fig. 3.4 signal space in transmitter and receiver.....	34
Fig. 4.1 Comparison of BER in different iteration number (I).....	41
Fig. 4.2 Comparison of BER in different speed (I).	42
Fig. 4.3 Comparison of BER in different group size (I).....	43
Fig. 4.4 Comparison of BER in different method (I).	44
Fig. 4.5 Comparison of BER in different speed and group size (I).....	45
Fig. 4.6 Comparison of BER in different group sizes with SD (I).....	46

Fig 4.7 Comparison of BER in different group sizes with LSD. 47

Fig. 4.8 Comparison of BER in different speed and group sizes with SD (I)..... 48

Fig. 4.9 Comparison of BER in different speed and group sizes with LSD (I). 49

Fig. 4.10 Comparison of BER in different numbers of iteration (II). 53

Fig. 4.11 Comparison of BER in different sizes of group (II). 54

Fig. 4.12 Comparison of BER in different $f_d T_s$ (II)..... 55

Fig. 4.13 Comparison of BER in LSD and SD (II)..... 56

Fig. 4.14 BER performance of group based method with perfect ICI cancellation (II). 57



Chapter 1

Introduction

OFDM is widely used in many wireless communication systems for high-bit-rate transmission over a frequency-selective fading channel. The concept of Orthogonal Frequency Division Multiplexing (OFDM) is initiated from that of multi-carriers systems [1] [2]. Data are transmitted through multiple carriers simultaneously to achieve high data rate transmission. In OFDM, the computationally efficient fast Fourier transform (FFT) is used to transmit data in parallel over a large number of orthogonal subcarriers. A cyclic prefix is inserted before each transmitted data block to eliminate the inter symbol interference (ISI). For time-invariant multipath channels, a single tap equalizer in frequency domain can be employed to recover the transmitted symbol on each subcarrier. However, due to the demand for orthogonality between each subcarrier, OFDM systems are sensitive to synchronization.

In high mobility environment, multipath channel is time varying. Channel variations may also arise the presence of an unknown carrier frequency offset, so the orthogonal property of OFDM is destroyed and result in the effect of inter-carrier interference among subcarriers which makes the performance of OFDM systems degrades severely [3] [4]. To reduce the ICI caused by channel variation, many approaches have been proposed, e.g.,

self-cancellation scheme [5], Sphere Decoding (SD) [6], minimum mean-squared error (MMSE) and MMSE with successive detection (MMSED) [7]. In [5], the method proposed sharpens the signal in frequency domain using the windowing operation in time domain to make subcarriers have approximate nulls around the location of other subcarriers and, therefore, creates less ICI. In [6], Sphere Decoding which solves the ML criterion is used to reduce the effect of ICI. In [7], it introduces a high performance equalization method by using MMSE with successive interference cancellation, but the computational complexity is very high.

According to Cai et al., [8] shows that ICI effect on a subcarrier comes from neighboring subcarriers, [9] and [10] propose a group based ICI cancellation method to lower the complexity and utilize successive ICI cancellation to get better performance. In this thesis, a parallel linked group based ICI cancellation method combined with Sphere Decoding or List Sphere Decoding is proposed to improve the system performance and lower the complexity of method in [6] which uses Sphere Decoding to reduce the ICI effect of OFDM system in high vehicle mobility environment. At the receiver, subcarriers are partitioned into several groups, each group uses SD or LSD to generate the message information and pass it to other groups for ICI cancellation. The operation of solving Sphere Decoding or List Sphere Decoding and passing message information for ICI cancellation will repeat iteratively to make performance better and better. In our proposed method, we assume that the channel state information are perfectly known at receiver.

The organization of this thesis is as following. In chapter 2, ICI effect on OFDM in high mobility environment, Sphere Decoding and List Sphere Decoding are introduced. In chapter 3, at first, the system model used in thesis is introduced then the group based ICI cancellation method with Sphere Decoding and List Sphere Decoding are introduced. In the end of the chapter 3, the parameter setting of Sphere Decoding is introduced. Computer simulation results along with some discussions are showed in chapter 4. Finally, in chapter 5, brier conclusions are made.



Chapter 2

OFDM System in High Mobility Environment and Sphere Decoding

2.1 High Mobility Environment

In wireless communication, received signals come from multiple paths due to reflection effects. Such environment is called a multipath channel. The equivalent baseband of a multipath channel impulse response can be described as [11]


$$h(t, \tau) = \sum_{l=0}^{L-1} a_l(t) \delta(t - \tau_l). \quad (2.1)$$

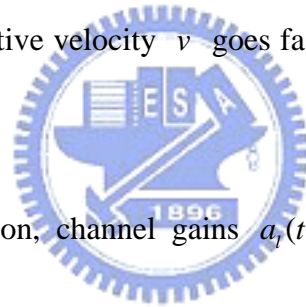
Where $a_l(t)$ and τ_l are the time-varying complex fading gain and the path delay of the l th path, L is the total number of multipath, and δ is the delta function. The variation speed of path gain $a_l(t)$ depends on maximal Doppler frequency or Doppler spread which is proportioned to the vehicle speed and carrier frequency. Maximal Doppler frequency is defined as eq. (2.2). The larger the Doppler spread is, the faster variation of the path gains are.

[12]

$$f_d = \frac{f_c v}{c}, \quad (2.2)$$

where f_c is the central frequency and v is the vehicle speed and c is the speed of light. In

OFDM system the parameter $f_d T_s$ is used to measure the effect of the ICI where T_s is the OFDM symbol period. We can observe that the inversion of T_s is the subchannel bandwidth and we can treat Doppler frequency as the frequency offset of a single tone signal after passing through the channel, so $f_d T_s$ is the fraction between frequency offset and subchannel bandwidth. If $f_d T_s$ is very small, it means that frequency offset relative to the subchannel bandwidth is too small which can be neglect, so the frequency of the signal can be seemed as the same as the original one. Otherwise, the mismatch of the frequency will occur at the receiver in OFDM systems. For fixed f_c and T_s , we can see from eq. (2.2) that f_d goes larger and larger when the relative velocity v goes faster and faster and it will cause the ICI effect goes severer and severer.



In the computer simulation, channel gains $a_r(t)$ are generated by Jakes model, the introduction of Jakes model is as following:

In the multipath Rayleigh fading channel without line of sight (LOS), the angel of the arrival signal in a plane is assumed to be uniformly distributed in the interval $[0, 2\pi)$. Jakes modeled the Rayleigh fading channel by a bank of oscillators with the maximal Doppler frequency and its fractions, as eq. (2.3) showed.

$$\begin{aligned} f_I(t) &= 2 \sum_{n=1}^{N_0} \cos \beta_n \cdot \cos \omega_n t + \sqrt{2} \cos \alpha \cdot \cos \omega_d t \\ f_Q(t) &= 2 \sum_{n=1}^{N_0} \sin \beta_n \cdot \cos \omega_n t + \sqrt{2} \sin \alpha \cdot \cos \omega_d t \end{aligned} \quad (2.3)$$

where

$$N = 2(2N_0 + 1), N_0 \geq 8$$

$$\omega_n = \omega_d \cos \alpha_n = \text{Doppler shifts}, n = 1, 2, \dots, N_0$$

$$\alpha_n = \frac{2\pi n}{N} = \text{the arrival angel of the } n\text{-th arrival signal}, n = 1, 2, \dots, N_0$$

$$\beta_n = \text{the phase of the } n\text{-th arrival signal}, n = 1, 2, \dots, N_0$$

In eq. (2.3), N_0 must be large enough to approximate to the central theorem. β_n are chosen properly such that the arrival phases are close to uniform distribution in $[0, 2\pi)$.

2.2 ICI on OFDM System

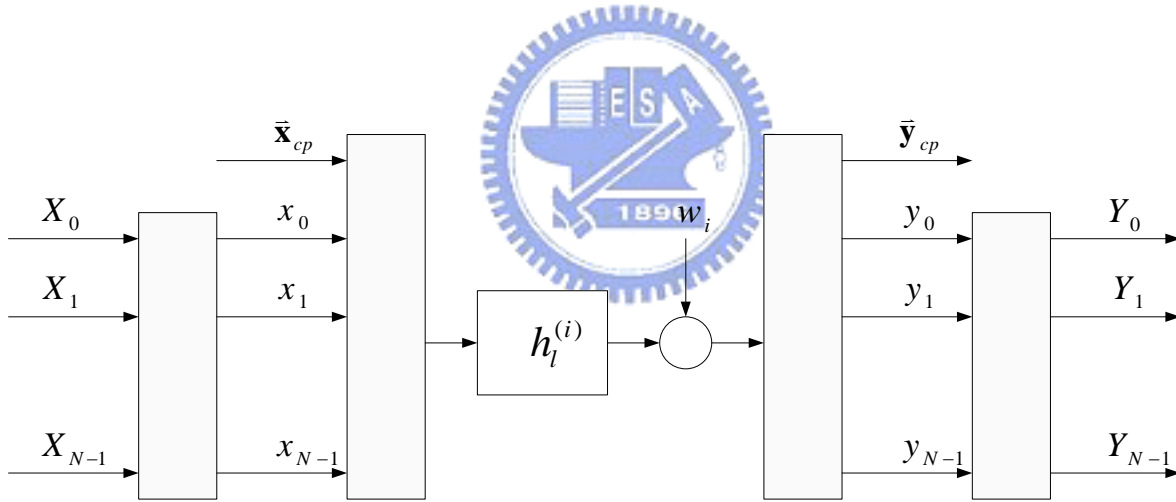


Fig. 2.1 Base-band OFDM System.

Fig 2.1 is the block diagram of base-band OFDM system. X_k , $k = 0, \dots, N-1$ the inputs of the Inverse Fast Fourier Transform (IFFT) represent the frequency domain data on the k -th subcarrier. x_k , $k = 0, \dots, N-1$ the outputs of the IFFT can be represented as follows :

$$x_i = \sum_{k=0}^{N-1} X_k e^{\frac{j2\pi ik}{N}} \quad 0 \leq i \leq N-1. \quad (2.4)$$

$\bar{\mathbf{x}}_{cp}$ represents the cyclic prefix (CP) with length N_G and is related to time domain sequence,

\mathbf{x} as follows :

$$\bar{\mathbf{x}}_{cp}(i) = x_{N-C+i} \quad 0 \leq i \leq N_G - 1. \quad (2.5)$$

Let T be the sampling period. Then $h_l^{(i)}$ is the l th channel tap at time instant $t = i \times T$. We

assume that the maximum delay spread of the channel is always less than or equal to N_G .

Then the channel output \mathbf{y} can be expressed as follows :

$$y_i = \sum_{l=0}^{N_G} h_l^{(i)} x_{((i-l))_N} + w_i \quad 0 \leq i \leq N-1. \quad (2.6)$$

In eq. (2.6), $((\))_N$ represents a cyclic shift in the base of N and w_i represents a sample of

additive white Gaussian noise. Then the fast Fourier transform (FFT) of sequence \mathbf{y} , will be

as follows :

$$Y_k = \sum_{i=0}^{N-1} y_i e^{-\frac{j2\pi ki}{N}} \quad 0 \leq k \leq N-1. \quad (2.7)$$

If $h_l^{(i)}$ is constant during one OFDM symbol time $(N+N_G) \times T$, then eq. (2.6)

becomes

$$y_i = \sum_{l=0}^{N_G} h_l x_{((i-l))_N} + w_i \quad 0 \leq i \leq N-1, \quad (2.8)$$

which is the circular convolution of \mathbf{h} and \mathbf{x} . By using eq. (2.7), eq. (2.4) and basic DFT

concept [13], we will find that the relationship between X_k and Y_k which is derived as

follows :

$$Y_k = \sum_{i=0}^{N-1} \left(\sum_{l=0}^{N_G} h_l x_{((i-l))_N} + w_i \right) e^{-\frac{j2\pi ki}{N}}$$

$$\begin{aligned}
&= \sum_{l=0}^{N_G} h_l \sum_{i=0}^{N-1} \left(x_{((i-l))_N} \right) e^{-\frac{j2\pi ki}{N}} + \sum_{i=0}^{N-1} w_i e^{-\frac{j2\pi ki}{N}} \\
&= \sum_{l=0}^{N_G} h_l \sum_{i=0}^{N-1} \sum_{n=0}^{N-1} X_n e^{-\frac{j2\pi((i-l))_N n}{N}} e^{-\frac{j2\pi ki}{N}} + W_k \\
&= \sum_{l=0}^{N_G} h_l \sum_{n=0}^{N-1} X_n \sum_{i=0}^{N-1} e^{-\frac{j2\pi((i-l))_N n}{N}} e^{-\frac{j2\pi ki}{N}} + W_k \\
&= \sum_{l=0}^{N_G} h_l \sum_{n=0}^{N-1} X_n e^{-\frac{j2\pi ln}{N}} \sum_{i=0}^{N-1} e^{-\frac{j2\pi in}{N}} e^{-\frac{j2\pi ki}{N}} + W_k \tag{2.9}
\end{aligned}$$

$$\begin{aligned}
&= \sum_{l=0}^{N_G} h_l \sum_{n=0}^{N-1} X_n e^{-\frac{j2\pi ln}{N}} \delta[n-k] + W_k \tag{2.10}
\end{aligned}$$

$$\begin{aligned}
&= X_k \sum_{l=0}^{N_G} h_l e^{-\frac{j2\pi lk}{N}} + W_k \\
&= H_k X_k + W_k. \tag{2.11}
\end{aligned}$$

Because of the orthogonal property of the subcarrier, we can derive eq. (2.9) to eq. (2.10). At

last, from eq. (2.11) we can see that Y_k only depends on X_k .

Unfortunately, impulse response of the channel is not a constant during one OFDM symbol time in high mobility environment. In section 2.1, we know that the channel impulse response is change in time, and frequency offset occurs due to the Doppler frequency. All the thing happened above destroy the orthogonal property of subcarriers. In this case, from eq.

(2.7) we can find that [14]

$$\begin{aligned}
Y_k &= \sum_{i=0}^{N-1} \left(\sum_{l=0}^{N_G} h_l^{(i)} x_{((i-l))_N} + w_i \right) e^{-\frac{j2\pi ki}{N}} \\
&= \sum_{l=0}^{N_G} \sum_{i=0}^{N-1} h_l^{(i)} x_{((i-l))_N} e^{-\frac{j2\pi ki}{N}} + \sum_{i=0}^{N-1} w_i e^{-\frac{j2\pi ki}{N}} \\
&= \sum_{l=0}^{N_G} \sum_{i=0}^{N-1} h_l^{(i)} x_{((i-l))_N} e^{-\frac{j2\pi ki}{N}} + W_k \\
&= \sum_{i=0}^{N-1} \sum_{l=0}^{N_G} h_l^{(i)} \left(\sum_{n=0}^{N-1} X_n e^{-\frac{j2\pi ln}{N}} e^{-\frac{j2\pi in}{N}} \right) e^{-\frac{j2\pi ki}{N}} + W_k \\
&= \sum_{n=0}^{N-1} X_n \sum_{l=0}^{N_G} \left(\sum_{i=0}^{N-1} h_l^{(i)} e^{-\frac{j2\pi(k-n)i}{N}} \right) e^{-\frac{j2\pi ln}{N}} + W_k
\end{aligned}$$

$$\begin{aligned}
&= \sum_{d=0}^{N-1} X_{((k-d))_N} \sum_{l=0}^{N_G} \left(\sum_{i=0}^{N-1} h_l^{(i)} e^{-\frac{j2\pi di}{N}} \right) e^{-\frac{j2\pi l(k-d)}{N}} + W_k \\
&= \left(\sum_{l=0}^{N_G} \sum_{i=0}^{N-1} h_l^{(i)} e^{-\frac{j2\pi lk}{N}} \right) X_k + \underbrace{\sum_{d=1}^{N-1} \left(\sum_{l=0}^{N_G} \left(\sum_{i=0}^{N-1} h_l^{(i)} e^{-\frac{j2\pi di}{N}} \right) e^{-\frac{j2\pi l(k-d)}{N}} \right)}_{ICI} X_{((k-d))_N} + W_k \\
&= \left(\sum_{l=0}^{N_G} \sum_{i=0}^{N-1} h_l^{(i)} e^{-\frac{j2\pi lk}{N}} \right) X_k + \underbrace{\sum_{d=1}^{N-1} \left(\sum_{l=0}^{N_G} F_l(d) e^{-\frac{j2\pi l(k-d)}{N}} \right)}_{ICI} X_{((k-d))_N} + W_k \\
&= H_{k,0} X_k + \underbrace{\sum_{d=1}^{N-1} H_{k,d} X_{((k-d))_N}}_{ICI} + W_k, \tag{2.12}
\end{aligned}$$

where

$$F_l(d) = \sum_{i=0}^{N-1} h_l^{(i)} e^{-\frac{j2\pi di}{N}}, 0 \leq l \leq N_G \ \& \ 0 \leq d \leq N-1. \tag{2.13}$$

Then $H_{k,d}$ can be defined as

$$H_{k,d} = \sum_{l=0}^{N_G} F_l(d) e^{-\frac{j2\pi l(k-d)}{N}} \quad 0 \leq k, d \leq N-1. \tag{2.14}$$

The second term of eq. (2.12) represents ICI which is the combination of other subcarriers and can't be neglected as the maximum Doppler frequency increases [15]. These ICI term causes the performance of OFDM degraded severely.

We treat eq. (2.13) as frequency response of the l th path and $H_{k,d}$ is the weight coefficient from the $((k-d))_N$ th subcarrier on the k th one. to the eq. Now, by the notion above, we try to explain why eq.(2.6) results in eq. (2.12). We can see from eq. (2.6) that at any time instant $t = i \times T$, the received signal y_i is the summation of the result of path coefficient multiply with delayed sample of OFDM symbol, so we can expect that subcarrier Y_k is the result of frequency response eq. (2.13) circular convolute with X_j , $0 \leq j \leq N-1$.

We use the notion above to rederive Y_k .

$$\begin{aligned}
Y_k &= FFT\{y_i\} \\
&= FFT\left\{\sum_{l=0}^{N_G} h_l x_{((i-l))_N} + w_i\right\} \\
&= \sum_{l=0}^{N_G} FFT\{h_l^{(i)} x_{((i-l))_N}\} + W_k \\
&= \sum_{l=0}^{N_G} FFT\{h_l^{(i)}\} \otimes FFT\{x_{((i-l))_N}\} + W_k \\
&= \sum_{l=0}^{N_G} F_l(k) \otimes X_k e^{-j\frac{2\pi lk}{N}} + W_k \\
&= \sum_{l=0}^{N_G} \sum_{d=0}^{N-1} F_l(d) X_{((k-d))_N} e^{-j\frac{2\pi l(k-d)}{N}} + W_k \\
&= \sum_{d=0}^{N-1} \sum_{l=0}^{N_G} F_l(d) e^{-j\frac{2\pi l(k-d)}{N}} X_{((k-d))_N} + W_k \\
&= \sum_{d=0}^{N-1} H_{k,d} X_{((k-d))_N} + W_k
\end{aligned}$$

We can find that the result of above equation is the same as eq.(2.12), so time variant channel causes frequency response and subcarrier do the circular convolution operation in OFDM systems.

2.3 Sphere Decoding

2.3.1 Real Sphere Decoding

In communication, Sphere Decoding (SD) [16], is used to solve the ML problem as

follows :

$$\hat{\mathbf{X}}_{ML} = \arg \min_{\mathbf{X} \in \Lambda} \|\mathbf{Y} - \mathbf{A}\mathbf{X}\|^2, \quad (2.15)$$

where \mathbf{A} is a M -by- N matrix where $M > N$, \mathbf{Y} is a N -by-1 vector, and \mathbf{X} is a N -by-1 vector. Λ is the set which includes all possible \mathbf{X} . We can derive from eq. (2.15) as follows :

$$\begin{aligned} \hat{\mathbf{X}}_{ML} &= \arg \min_{\mathbf{X} \in \Lambda} \|\mathbf{Y} - \mathbf{A}\mathbf{X}\|^2 \\ &= \arg \min_{\mathbf{X} \in \Lambda} (\mathbf{Y} - \mathbf{A}\mathbf{X})^T (\mathbf{Y} - \mathbf{A}\mathbf{X}) \\ &= \arg \min_{\mathbf{X} \in \Lambda} \mathbf{Y}^T \mathbf{Y} - \mathbf{Y}^T \mathbf{A}\mathbf{X} - \mathbf{X}^T \mathbf{A}^T \mathbf{Y} + \mathbf{X}^T \mathbf{A}^T \mathbf{A}\mathbf{X} \\ &= \arg \min_{\mathbf{X} \in \Lambda} \left(\mathbf{Y}^T \mathbf{A} (\mathbf{A}^T \mathbf{A})^{-1} \mathbf{A}^T \mathbf{Y} - \mathbf{Y}^T \mathbf{A}\mathbf{X} - \mathbf{X}^T \mathbf{A}^T \mathbf{Y} + \mathbf{X}^T \mathbf{A}^T \mathbf{A}\mathbf{X} \right) + \\ &\quad \left(\mathbf{Y}^T \mathbf{Y} - \mathbf{Y}^T \mathbf{A} (\mathbf{A}^T \mathbf{A})^{-1} \mathbf{A}^T \mathbf{Y} \right) \\ &= \arg \min_{\mathbf{X} \in \Lambda} \left(\mathbf{Y}^T \mathbf{A} (\mathbf{A}^T \mathbf{A})^{-1} \mathbf{I} \mathbf{A}^T \mathbf{Y} - \mathbf{Y}^T \mathbf{A}\mathbf{X} - \mathbf{X}^T \mathbf{I} \mathbf{A}^T \mathbf{Y} + \mathbf{X}^T \mathbf{A}^T \mathbf{A}\mathbf{X} \right) + \mathbf{Y}^T \left(\mathbf{I} - \mathbf{A} (\mathbf{A}^T \mathbf{A})^{-1} \mathbf{A}^T \right) \mathbf{Y} \\ &= \arg \min_{\mathbf{X} \in \Lambda} \left(\mathbf{Y}^T \mathbf{A} (\mathbf{A}^T \mathbf{A})^{-1} (\mathbf{A}^T \mathbf{A}) (\mathbf{A}^T \mathbf{A})^{-1} \mathbf{A}^T \mathbf{Y} - \right. \\ &\quad \left. \mathbf{Y}^T \mathbf{A} (\mathbf{A}^T \mathbf{A})^{-1} (\mathbf{A}^T \mathbf{A}) \mathbf{X} - \mathbf{X}^T (\mathbf{A}^T \mathbf{A}) (\mathbf{A}^T \mathbf{A})^{-1} \mathbf{A}^T \mathbf{Y} + \mathbf{X}^T \mathbf{A}^T \mathbf{A}\mathbf{X} \right) + \\ &\quad \mathbf{Y}^T \left(\mathbf{I} - \mathbf{A} (\mathbf{A}^T \mathbf{A})^{-1} \mathbf{A}^T \right) \mathbf{Y} \\ &= \arg \min_{\mathbf{X} \in \Lambda} \left(\mathbf{Y}^T (\mathbf{A}^\dagger)^T \mathbf{A}^T \mathbf{A} \mathbf{A}^\dagger \mathbf{Y} - \mathbf{Y}^T (\mathbf{A}^\dagger)^T \mathbf{A}^T \mathbf{A}\mathbf{X} - \mathbf{X}^T \mathbf{A}^T \mathbf{A} \mathbf{A}^\dagger \mathbf{Y} + \mathbf{X}^T \mathbf{A}^T \mathbf{A}\mathbf{X} \right) + \\ &\quad \mathbf{Y}^T \left(\mathbf{I} - \mathbf{A} (\mathbf{A}^T \mathbf{A})^{-1} \mathbf{A}^T \right) \mathbf{Y} \\ &= \arg \min_{\mathbf{X} \in \Lambda} \left(\mathbf{A} (\mathbf{A}^\dagger \mathbf{Y} - \mathbf{X}) \right)^T \left(\mathbf{A} (\mathbf{A}^\dagger \mathbf{Y} - \mathbf{X}) \right) + \mathbf{Y}^T \left(\mathbf{I} - \mathbf{A} (\mathbf{A}^T \mathbf{A})^{-1} \mathbf{A}^T \right) \mathbf{Y} \\ &= \arg \min_{\mathbf{X} \in \Lambda} \left(\hat{\mathbf{X}} - \mathbf{X} \right)^T \mathbf{A}^T \mathbf{A} \left(\hat{\mathbf{X}} - \mathbf{X} \right) + \alpha. \end{aligned} \quad (2.16)$$

In eq. (2.16), α is a constant and does not change when different \mathbf{X} is chosen.

$\mathbf{A}^\dagger = (\mathbf{A}^T \mathbf{A})^{-1} \mathbf{A}^T$ is the pseudo inverse of \mathbf{A} , so $\hat{\mathbf{X}}$ is the least square solution of $\mathbf{A}\mathbf{X} = \mathbf{Y}$. As the same as [17], to solve eq (2.15) is equivalent to solve as follows :

$$\hat{\mathbf{X}}_{ML} = \arg \min_{\mathbf{X} \in \Lambda} \left(\hat{\mathbf{X}} - \mathbf{X} \right)^T \mathbf{A}^T \mathbf{A} \left(\hat{\mathbf{X}} - \mathbf{X} \right). \quad (2.17)$$

The easiest way to solve eq. (2.17) is to check all the possible of \mathbf{X} and finds which one of

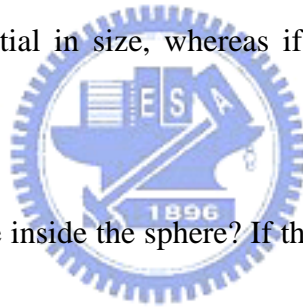
\mathbf{X} causes the minimum. However, the computational complexity of above exhaustive search method is really high So sphere decoding is brought up to avoid the exhaustive search and searches only over the possible \mathbf{X} which lies in a certain sphere centered at the given vector with radius r . In this notion eq. (2.18) can be written as follows in Sphere decoding

$$\hat{\mathbf{X}}_{ML} = \arg \min_{\mathbf{X} \in \Lambda} \left(\hat{\mathbf{X}} - \mathbf{X} \right)^T \mathbf{A}^T \mathbf{A} \left(\hat{\mathbf{X}} - \mathbf{X} \right) \leq r^2 . \quad (2.18)$$

It is clear that the closest point inside the sphere will also be the closest point for the whole point. However, close scrutiny of this basic ideal leads to two key questions [16].

1) How do you choose radius r ? Clearly, if radius is too large, we obtain too many points,

and the search remains exponential in size, whereas if radius too small, we obtain no points inside the sphere.



2) How can we tell which points are inside the sphere? If this requires testing the distance of each point from $\hat{\mathbf{X}}$, then there is no point in sphere decoding, as we will still need an exhaustive search.

Sphere decoding does not really address the first question. However it does propose an efficient way to answer the second. The basic observation is the following. Although it is difficult to determine the points inside a general N -dimensional sphere, it is trivial to do so in the one-dimensional case. The reason is that a one-dimensional sphere reduces to the endpoints of an interval, and so, the desired points will be the integer values that lie in this interval. We can use this observation to go from dimension k to dimension $k+1$. Suppose that

we have determined all k -dimensional points that lie in a sphere of radius r . Then, for any such k -dimensional points, the set of admissible values of the $(k+1)$ th dimensional coordinate that lie in the higher dimensional sphere of the same radius forms an interval. So we can determine all points in a sphere of dimension N and radius r by successively determining all points in spheres of lower dimensions $1, \dots, N$ and the same radius r .

In eq. (2.18), we choose the least square solution as the center of sphere which is the optimum unconstrained solution in this problem. As Fig 2.2 we will find the minimal solution lies in the sphere with radius r .

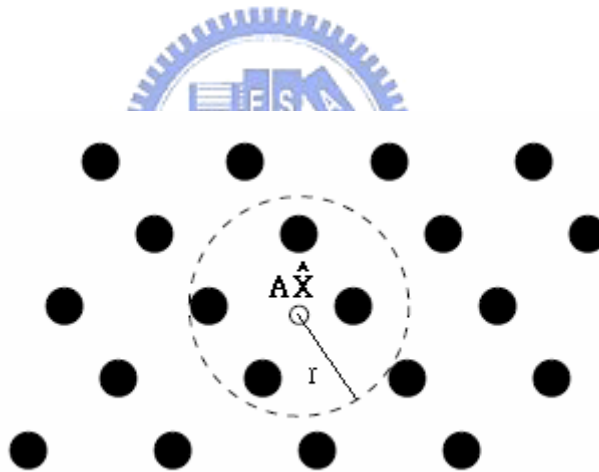


Fig. 2.2 A sphere of radius r and centered at $\mathbf{A}\hat{\mathbf{X}}$.

To solve this problem efficiently Cholesky factorization is employed to find an upper triangular \mathbf{U} with u_{ii} real and positive such that $\mathbf{U}^T\mathbf{U} = \mathbf{A}^T\mathbf{A}$. So eq. (2.18) can be written as

$$\hat{\mathbf{X}}_{ML} = \arg \min_{\mathbf{X} \in \Lambda} (\hat{\mathbf{X}} - \mathbf{X})^T \mathbf{U}^T \mathbf{U} (\hat{\mathbf{X}} - \mathbf{X}) \leq r^2$$

$$\begin{aligned}
&= \arg \min_{\mathbf{X} \in \Lambda} \mathbf{D}^T \mathbf{D} \quad \text{where } \mathbf{D} = \mathbf{U}(\hat{\mathbf{X}} - \mathbf{X}) \\
&= \sum_{i=1}^N d_i^2 \quad \text{where } d_i = \sum_{j=i}^N u_{ij} (X_j - \hat{X}_j) \text{ and } u_{ij} = 0, \text{ for } i < j \\
&= \arg \min_{\mathbf{X} \in \Lambda} \sum_{i=1}^N \left[u_{ii} (X_i - \hat{X}_i) + \sum_{j=i+1}^N u_{ij} (X_j - \hat{X}_j) \right]^2 \leq r^2 \\
&= \arg \min_{\mathbf{X} \in \Lambda} \sum_{i=1}^N u_{ii}^2 \left[X_i - \hat{X}_i + \sum_{j=i+1}^N \frac{u_{ij}}{u_{ii}} (X_j - \hat{X}_j) \right]^2 \leq r^2. \tag{2.19}
\end{aligned}$$

In eq. (2.19), the sphere decoder establishes bounds on X_1, \dots, X_N by examining these terms in subsets.

Starting with $i = N$, and throwing out the terms $i = 1, \dots, N-1$, we obtain from eq.

(2.19)

$$\begin{aligned}
&u_{NN}^2 (X_N - \hat{X}_N)^2 \leq r^2 \\
\Rightarrow &\left\lceil \hat{X}_N - \frac{r}{u_{NN}} \right\rceil \leq X_N \leq \left\lfloor \hat{X}_N + \frac{r}{u_{NN}} \right\rfloor. \tag{2.20}
\end{aligned}$$

($\lceil \cdot \rceil$ and $\lfloor \cdot \rfloor$ means the ceiling function and the floor function operators return the smallest integer greater than or equal to, and the largest integer less than or equal to their respective arguments; these functions are applied in the case which the constellation is a set of consecutive integers such as QPSK or QAM.) After computing the lower and upper bounds in eq. (2.20), the sphere decoder chooses a candidate value for X_N and computes the implication of this choice on X_{N-1} . To find the influence of the choice of \hat{X}_N and \hat{X}_{N-1} the sphere decoder looks at the two terms $i = M-1$ in eq. (2.19), throws out the remaining terms, and obtains the inequality

$$u_{N-1,N-1}^2 \left[X_{N-1} - \hat{X}_{N-1} + \frac{u_{N-1,N}}{u_{NN}} (X_N - \hat{X}_N) \right]^2 + u_{NN}^2 (X_N - \hat{X}_N)^2 \leq r^2$$

which yields the upper bound

$$X_{N-1} \leq \left[\hat{X}_{N-1} + \frac{\sqrt{r^2 - u_{NN}^2 (X_N - \hat{X}_N)^2}}{u_{N-1,N-1}} - \frac{u_{N-1,N}}{u_{NN}} (X_N - \hat{X}_N) \right]$$

and the lower bound

$$X_{N-1} \geq \left[\hat{X}_{N-1} - \frac{\sqrt{r^2 - u_{NN}^2 (X_N - \hat{X}_N)^2}}{u_{N-1,N-1}} - \frac{u_{N-1,N}}{u_{NN}} (X_N - \hat{X}_N) \right].$$

The sphere decoder now chooses a candidate for X_{N-1} within the range given by the upper and lower bounds, and proceeds to X_{N-2} , and so on.

There are two things happen during the algorithm operating.

- 1) The decoder reaches X_1 and chooses a value within the computed range.
- 2) The decoder finds that no point in the constellation fall within the upper and lower bounds obtained for some X_j .

In the first case, the sphere decoder has a candidate solution for the entire vector \mathbf{X} , computes its radius which cannot exceed r , and starts the search process over, using this new smaller radius to find any better candidates. In the second case, the decoder must have made at least one bad candidate choice for X_{j+1}, \dots, X_N . The decoder revises the choice for X_{j+1} which immediately preceded the attempt for X_j by finding another candidate value within its range, and proceeds again to try X_j . If no more candidates are available at X_{j+1} , the

decoder backtracks to X_{j+2} , and so on.

The algorithm for determining the points in an N-dimensional sphere essentially constructs a tree in Sphere Decoding (see Fig 2.3). Let's use this tree structure to briefly explain the operation of Sphere Decoding.

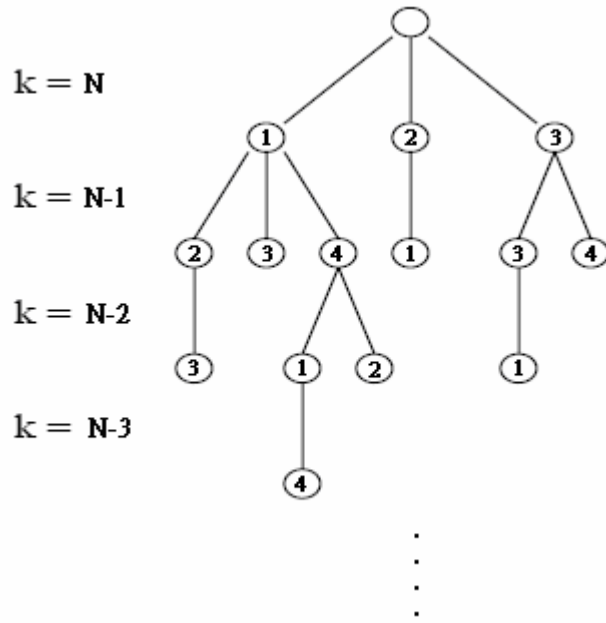


Fig. 2.3 Sample tree generated to determine points in a N-dimensional sphere.

The node at the top of the fig. 2.3 is treated as the start node and others with numbers inside represent the point in the set S where S^N is equal to Λ (take BPSK as an example, $S = \{-1,1\}$). Choosing different node at layer N makes eq. (2.19) generates different upper and lower bound for layer N-1, so the nodes can be chosen at layer N-1 depend on the node which is chosen at the layer N. Now, if node choosing order from layer N to N-2 is 1、2、3, then we can find that there is no node can be chosen at layer N-3. So the algorithm backs to layer N-2 and unfortunately, there is still no node (excluding 3, because it has been chosen)

can be chosen. Then the algorithm backs again and goes to layer N-1. At this layer, it remains two nodes (excluding 2) can be chosen, so 3 is chosen and algorithm keep going until it finishes the choosing operation at layer 1. After finishing the choosing operation at layer 1, a feasible solution is generated and this point will be used to generate a new radius. New radius replaces the initial radius for generating the upper and lower bound of every layer, so algorithm keeps going with new lower and upper bound at layer 1. Under this procedure, the tree structure may change again and again that is the sphere becomes smaller and smaller. If the algorithm is terminated, the last feasible solution is the best solution.

2.3.2 Complex Sphere Decoding



The Sphere Decoding algorithm described above applies on a real system where \mathbf{X} is chosen from a real lattice, but in communication systems we face to deal with complex system because of the modulation scheme we used such as QPSK. In this case, eq. (2.18) becomes as follows :

$$\hat{\mathbf{X}}_{ML} = \arg \min_{\mathbf{X} \in \Lambda} (\hat{\mathbf{X}} - \mathbf{X})^H \mathbf{A}^H \mathbf{A} (\hat{\mathbf{X}} - \mathbf{X}) \leq r^2 \quad (2.21)$$

where \mathbf{A} , \mathbf{X} , and $\hat{\mathbf{X}}$ are complex value. Here two kinds of methods are introduced to deal with this problem. The first method applies the algorithm on the complex system by decoupling the real and imaginary components of $\hat{\mathbf{X}}$, \mathbf{A} , and \mathbf{X} to create a system of real

equations with twice the dimension of the original system [18]. For example, eq. (2.21) can be transformed into a real equation in matrix form as follows

$$\tilde{\mathbf{X}}_{ML} = \arg \min_{\tilde{\mathbf{X}} \in \tilde{\Lambda}} (\tilde{\mathbf{X}}_{LS} - \tilde{\mathbf{X}})^T \tilde{\mathbf{A}}^T \tilde{\mathbf{A}} (\tilde{\mathbf{X}}_{LS} - \tilde{\mathbf{X}}) \leq r^2 \quad (2.22)$$

where

$$\tilde{\mathbf{X}} = \begin{bmatrix} \text{Re}\{\mathbf{X}^T\} & -\text{Im}\{\mathbf{X}^T\} \end{bmatrix}$$

$$\tilde{\mathbf{X}}_{LS} = \begin{bmatrix} \text{Re}\{\hat{\mathbf{X}}^T\} & -\text{Im}\{\hat{\mathbf{X}}^T\} \end{bmatrix}$$

$$\tilde{\mathbf{A}} = \begin{bmatrix} \text{Re}\{\mathbf{A}^T\} & -\text{Im}\{\mathbf{A}^T\} \\ \text{Im}\{\mathbf{A}^T\} & \text{Re}\{\mathbf{A}^T\} \end{bmatrix}$$

and $\tilde{\Lambda} = \{\text{Re}(\Lambda), \text{Im}(\Lambda)\}$. If \mathbf{X} belongs to QPSK then each entry of $\tilde{\mathbf{X}}$ belongs to BPSK.

Thus eq. (2.22) can be solved via SD which we introduced in section 2.3.1.

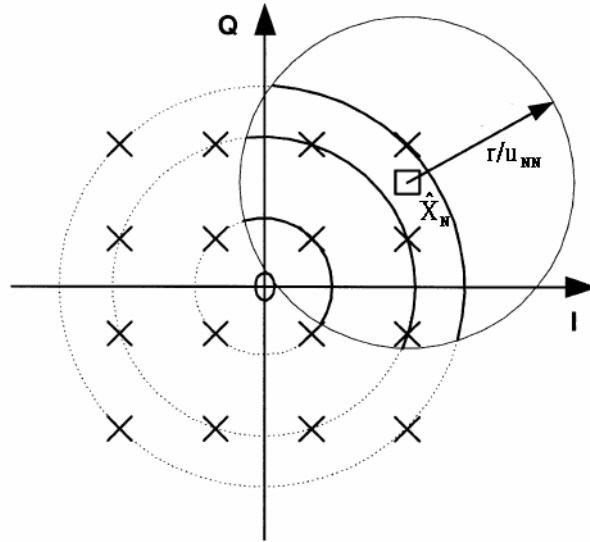


Fig. 2.4 Searching disk in 16-QAM.

The second method [19] uses eq. (2.21) directly without decoupling, but the searching domain

Λ is not integer set anymore (see Fig 2.4). As the same as eq. (2.19) we can derive from eq.

(2.21) as follows

$$\begin{aligned}\hat{\mathbf{X}}_{ML} &= \arg \min_{\mathbf{X} \in \Lambda} (\hat{\mathbf{X}} - \mathbf{X})^H \mathbf{U}^H \mathbf{U} (\hat{\mathbf{X}} - \mathbf{X}) \leq r^2 \\ &= \arg \min_{\mathbf{X} \in \Lambda} \sum_{i=1}^N u_{ii}^2 \left[X_i - \hat{X}_i + \sum_{j=i+1}^N \frac{u_{ij}}{u_{ii}} (X_i - \hat{X}_i) \right]^2 \leq r^2\end{aligned}\quad (2.23)$$

As the real case, Sphere Decoding algorithm starts at $i = N$ and lets $X_N = r_c e^{i\theta_N}$ and

$\hat{X}_N = \hat{r}_c e^{i\hat{\theta}_N}$, where

$$\theta_k \in \left\{ 0, \frac{2\pi}{2^{M_c}}, \dots, \frac{2\pi(2^{M_c} - 1)}{2^{M_c}} \right\} \quad (2.24)$$

M_c is the number of bits per symbol, for example $M_c = 2$ for QPSK. Then, we get

$$\begin{aligned}|X_N - \hat{X}_N|^2 &= r_c^2 + \hat{r}_c^2 - 2r_c \hat{r}_c \cos(\theta_N - \hat{\theta}_N) \leq \frac{r^2}{u_{NN}^2} \\ \Rightarrow \cos(\theta_N - \hat{\theta}_N) &\geq \frac{1}{2r_c \hat{r}_c} \left[r_c^2 + \hat{r}_c^2 - \frac{r^2}{u_{NN}^2} \right] =: \eta\end{aligned}\quad (2.25)$$

$$\Rightarrow \left[\frac{2^{M_c}}{2\pi} (\hat{\theta}_N - \cos^{-1} \eta) \right] \leq \frac{2^{M_c}}{2\pi} \theta_N \leq \left[\frac{2^{M_c}}{2\pi} (\hat{\theta}_N + \cos^{-1} \eta) \right]. \quad (2.26)$$

We can see from eq. (2.26) the searching domain change to eq. (2.24) now. From eq. (2.26),

if $\eta > 1$, then the search disk does not contain any point of the constellation (because the

range of cosine function is $[-1, 1]$, it is impossible to find a value makes $\cos(\theta_N - \hat{\theta}_N) > 1$). If

$\eta < -1$, then the search disk includes the entire constellation ($\cos(\theta_N - \hat{\theta}_N) > -1$ is always

right no what value is in the cosine function). For M-QAM there are different values of r_c , so

solving for the points within the search disk simply requires solving the inequality eq. (2.25)

for different values of r_c , or decoupling the M-QAM to multiple QPSK [20]. To simplify the

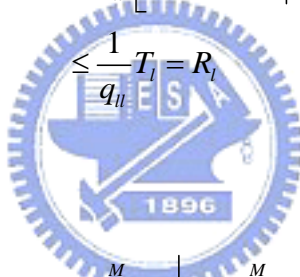
computing of the algorithm, the recursive equations is develop [19]. Let $\xi_i = \hat{X}_i - X_i$,

$q_{ii} = u_{ii}^2$, $q_{ij} = u_{ij} / u_{ii}$ and substitute into eq. (2.23) gets

$$\sum_{i=1}^N q_{ii} \left| \xi_i + \sum_{j=i+1}^N q_{ij} \xi_j \right|^2 \leq r^2 .$$

For $k = l$,

$$\begin{aligned} & q_{ll} \left| \xi_l + \sum_{j=l+1}^K q_{lj} \xi_j \right|^2 + \sum_{i=l+1}^K q_{ii} \left| \xi_i + \sum_{j=i+1}^K q_{ij} \xi_j \right|^2 \leq r^2 \\ \Rightarrow & \left| \xi_l + \sum_{j=l+1}^K q_{lj} \xi_j \right|^2 \leq \frac{1}{q_{ll}} \left[r^2 - \sum_{i=l+1}^K q_{ii} \left| \xi_i + \sum_{j=i+1}^K q_{ij} \xi_j \right|^2 \right] \\ \Rightarrow & |\hat{s}_l - s_l + S_l|^2 \leq \frac{1}{q_{ll}} \left[r^2 - \sum_{i=l+1}^K q_{ii} \left| \xi_i + \sum_{j=i+1}^K q_{ij} \xi_j \right|^2 \right] \end{aligned}$$



where

$$\begin{aligned} T_i &= r^2 - \sum_{l=i+1}^M q_{ll} \left| \xi_l + \sum_{j=l+1}^M q_{lj} \xi_j \right|^2 \\ R_i &= \frac{1}{q_{ii}} \left(r^2 - \sum_{l=i+1}^M q_{ll} \left| \xi_l + \sum_{j=l+1}^M q_{lj} \xi_j \right|^2 \right) \\ R_i &= \frac{T_i}{q_{ii}} . \end{aligned}$$

Let $s'_i = \hat{s}_i + S_i = r'_{c,i} e^{j\theta_i}$, $S_i = \sum_{j=i+1}^M q_{ij} \xi_j$, we can get

$$T_i = T_{i+1} - q_{i+1,i+1} \left| \xi_{i+1} + S_{i+1} \right|^2, \quad (2.27)$$

and the i th summation term in eq. (2.23) can be written as follows :

$$\left| s'_i - s_i \right|^2 = r_c^2 + r_{c,i}^2 - 2r_c r'_{c,i} \cos(\theta_i - \theta'_i) \leq R_i$$

$$\cos(\theta_i - \theta'_i) \geq \frac{1}{2r_c r_{c,i}} [r_c^2 + r_{c,i}^2 - R_i] = \eta_i \quad (2.28)$$

$$\left[\frac{2^{M_c}}{2\pi} (\theta'_i - \cos^{-1} \eta_i) \right] \leq \frac{2^{M_c}}{2\pi} \theta_i \leq \left[\frac{2^{M_c}}{2\pi} (\theta'_i + \cos^{-1} \eta_i) \right]. \quad (2.29)$$

The distance between point $\mathbf{A}\hat{\mathbf{X}}$ and obtained point by Sphere Decoding in received signal domain can be computed by the formula below :

$$d^2 = T_K - T_0 = T_K - T_1 + q_{11} |\xi_1 + S_1|^2. \quad (2.30)$$

For every stage, eq. (2.27) is used to compute the parameter which is needed in eq. (2.28) and eq. (2.29) to calculate the upper and lower bound of next stage. The second method is easy to use in computer programming, so it is adopted in this thesis.

2.4 List Sphere Decoding



List Sphere decoding (LSD) is modified from sphere decoding [17]. LSD gives a list L which contains N_{cand} candidates of \mathbf{X} with smaller values in eq. (2.15) for generating the soft information. In order to generate L , the sphere decoder needs to be modified in two ways. Every time it finds a point inside the initial radius r :

- 1) it does not decrease r to correspond to the radius of this new point;
- 2) adding this point to L if the list is not full; or if L is full, it compares this point with the point in L with the largest radius and replaces this point if the new point has smaller radius.

By the changes above, List Sphere Decoding searches all the points which are inside of the sphere with given initial radius, and gives the N_{cand} best point. Sphere Decoding changes to search the point in new sphere (the center of the sphere is still the same) when its find a new point whose distance to the center of the sphere is smaller than initial radius (mentioned in section 2.3.1). So the points which are inside the old sphere and outside the new sphere will not be considered in Sphere Decoding and the searching tree of SD goes smaller and smaller (actually, another smaller tree) which is not the case in LSD. The searching tree of LSD is still the same and all the branches must be gone through.

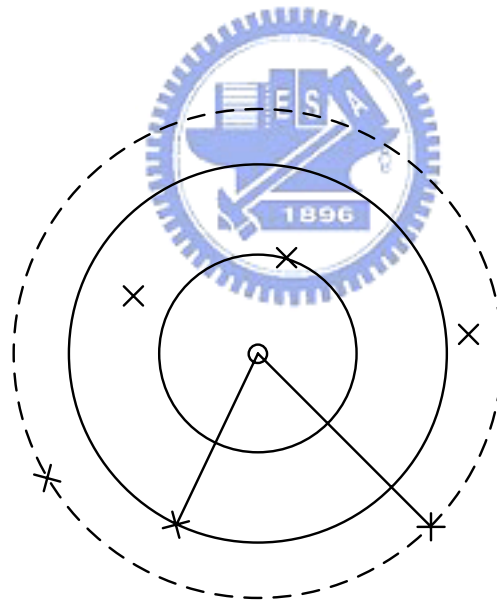


Fig. 2.5 Sphere of SD or LSD in received signal domain.

Here, we use Fig. 2.5 to explain the different between SD and LSD. In Fig.2.5, the circle mark represents the center of the sphere and cross mark means the feasible solution in received signal domain where the number beside of them is used to indicate. For SD with

initial radius r_1 , if the cross mark 4 is first found and radius r_2 is used to be the new radius of the searching tree then cross mark 1, 2 and 3 will not be presented in new searching tree with radius r_2 . Again, if the cross mark 6 is found in the new searching tree with radius r_2 then cross mark 5 will not be considered for next searching tree. However, for LSD with initial radius r_1 , if the cross mark 4 is first found, cross mark 1, 2, 3, 5, 6 are still in the searching trees with radius r_1 because LSD will not change the radius. Back to fig. 2.3, when LSD finishes the searching operation at layer 1 successfully, it puts this point into the list, backs to layer 2, and keeps the algorithm going. Then all the feasible points in the sphere will be found out successively (the finding order is independent of the distance to the center of the sphere).



Chapter 3

Grouped Based ICI Cancellation Method

3.1 System Model

In section 2.2, we have known the ICI effect on OFDM systems and its mathematic representation. Now, we change the mathematic representation in section 2.2 into matrix form which is convenient to be used in proposed method. Eq. (2.12) can be rewrote as follows :


$$\mathbf{x} = \mathbf{F}_N^H \mathbf{X} \quad (3.1)$$

where $\mathbf{x} = [x_0, \dots, x_{N-1}]^T$, $\mathbf{X} = [X_0, \dots, X_{N-1}]^T$ as showed in Fig. 2.1 and \mathbf{F}_N is the N point FFT matrix which can be represented as follows :

$$\mathbf{F}_N = \begin{bmatrix} e^{-j\frac{2\pi 0 \cdot 0}{N}} & e^{-j\frac{2\pi 0 \cdot 1}{N}} & \dots & e^{-j\frac{2\pi 0 \cdot (N-2)}{N}} & e^{-j\frac{2\pi 0 \cdot (N-1)}{N}} \\ e^{-j\frac{2\pi 1 \cdot 0}{N}} & & & & e^{-j\frac{2\pi 1 \cdot (N-1)}{N}} \\ \vdots & & \ddots & & \vdots \\ e^{-j\frac{2\pi (N-2) \cdot 0}{N}} & & & & e^{-j\frac{2\pi (N-2) \cdot (N-1)}{N}} \\ e^{-j\frac{2\pi (N-1) \cdot 0}{N}} & e^{-j\frac{2\pi (N-1) \cdot 1}{N}} & \dots & e^{-j\frac{2\pi (N-1) \cdot (N-2)}{N}} & e^{-j\frac{2\pi (N-1) \cdot (N-1)}{N}} \end{bmatrix} \quad (3.2)$$

Assume that the maximum delay spread of the channel always less than or equal to the length of cyclic prefix be used, so the received signal $\mathbf{y} = [y_0, \dots, y_{N-1}]^T$ and its FFT becomes :

$$\mathbf{y} = \mathbf{H}\mathbf{x} + \mathbf{w} \quad (3.3)$$

$$\begin{aligned} \mathbf{Y} &= \mathbf{F}_N \mathbf{y} \\ &= \mathbf{F}_N \mathbf{H}\mathbf{x} + \mathbf{W} \\ &= \mathbf{A}\mathbf{X} + \mathbf{W} \end{aligned} \quad (3.4)$$

with \mathbf{w} is an $N \times 1$ AWGN noise and $\mathbf{A} = \mathbf{F}_N \mathbf{H} \mathbf{F}_N^H$. The channel impulse response matrix

\mathbf{H} is defined as follow [21]

$$\mathbf{H} = \begin{bmatrix} h_0^{(0)} & 0 & \dots & 0 & h_{L-1}^{(0)} & \dots & h_1^{(0)} \\ \vdots & \ddots & \ddots & \ddots & \ddots & \ddots & \vdots \\ h_{L-1}^{(L-1)} & h_{L-2}^{(L-1)} & \dots & h_0^{(L-1)} & 0 & \dots & 0 \\ 0 & \ddots & \ddots & \ddots & \ddots & \ddots & \vdots \\ \vdots & \ddots & \ddots & \ddots & \ddots & \ddots & 0 \\ 0 & \dots & 0 & h_{L-1}^{(N-1)} & \dots & h_0^{(N-1)} \end{bmatrix} \quad (3.5)$$

where $h_k^{(i)}$ is the k -th channel tap at time instant $t = i \times T$ and T is the sampling period.

Now, we want to find a $\hat{\mathbf{X}}$ such that

$$\hat{\mathbf{X}} = \arg \min_{\mathbf{X} \in \Lambda} \|\mathbf{Y} - \mathbf{A}\mathbf{X}\|^2 \quad (3.6)$$

where Λ is the set includes all possible of \mathbf{X} . Clearly, we can apply Sphere Decoding to solve eq. (3.6) [6], but the complexity of this method is very large.

3.2 Group based ICI Cancellation Method with Sphere Decoding

From [8], we know that most of the ICI effect on a subcarrier comes from neighboring

subcarriers, so we assume the window length of the ICI effect is $Q=2q+1$ that is X_i causes interference to $Y_{((i-q))_N} \sim Y_{((i+q))_N}$. Let $\mathbf{X}_i = [X_{iN_x}, \dots, X_{(i+1)N_x-1}]^T$ be a segment of \mathbf{X} and for any $i \neq j$, $\mathbf{X}_i \cap \mathbf{X}_j = \{0\}$ where N_x is the size of one segment. Accordingly, \mathbf{X}_i will induce the interference on $\mathbf{Y}_i = [Y_{((i-N_x-q))_N}, \dots, Y_{iN_x}, \dots, Y_{((i+1)N_x-1+q)_N}]^T$. From Fig 3.1, \mathbf{Y}_i also suffers the interference from \mathbf{X}_{i-1} and \mathbf{X}_{i+1} or even more segments (depend on how large N_x and q are), so performance of solving \mathbf{X}_i by \mathbf{Y}_i directly may not be acceptable.

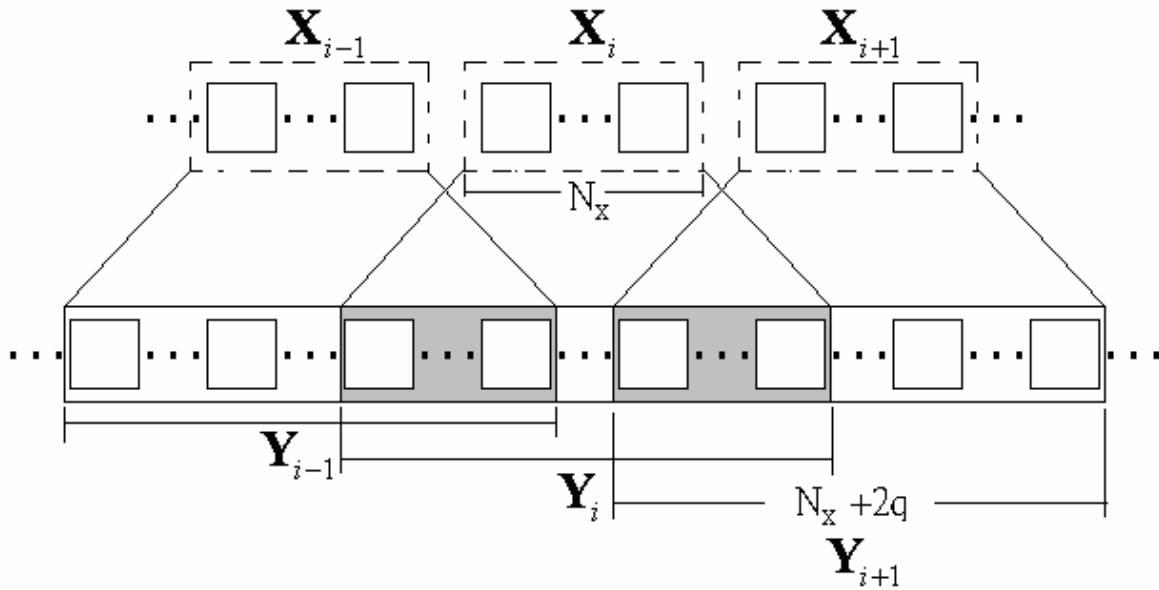


Fig. 3.1 Group Method for ICI with window length $Q=2q+1$.

The basic ideal of our method is to cancel the component of \mathbf{X}_j , $i \neq j$ in \mathbf{Y}_i . Again, from [8], most of the ICI effect on a subcarrier comes from neighboring subcarriers. We use $n_x > 2q-1$ so that \mathbf{Y}_i is affected by \mathbf{X}_{i-1} , \mathbf{X}_i and \mathbf{X}_{i+1} only. The relationship of \mathbf{Y}_i , \mathbf{X}_{i-1} , \mathbf{X}_i and \mathbf{X}_{i+1} can be represented as follows :

$$\mathbf{Y}_i = [\mathbf{A}_{i-1}^i] \mathbf{X}_{i-1} + [\mathbf{A}_i^i] \mathbf{X}_i + [\mathbf{A}_{i+1}^i] \mathbf{X}_{i+1} \quad (3.7)$$

where

$$[\mathbf{A}_i^j] = \begin{bmatrix} a_{((j \cdot n_x - q))_N, i \cdot n_x} & \cdots & a_{((j \cdot n_x - q))_N, (i+1)n_x - 1} \\ \vdots & \ddots & \vdots \\ a_{(((j+1)n_x - 1 + q))_N, i \cdot n_x} & \cdots & a_{(((j+1)n_x - 1 + q))_N, (i+1)n_x - 1} \end{bmatrix} \quad (3.8)$$

a_{ij} is the element of \mathbf{A} on i -th row and j -th column in eq. (3.4). First, solving \mathbf{X}_i , \mathbf{X}_{i-1} and \mathbf{X}_{i+1} individually by \mathbf{Y}_i , \mathbf{Y}_{i-1} and \mathbf{Y}_{i+1} by using Sphere Decoding. Eq. (2.21) applied here becomes as follow :

$$\hat{\mathbf{X}}_{i,ML} = \arg \min_{\mathbf{X}_i \in \Lambda} (\hat{\mathbf{X}}_i - \mathbf{X}_i)^H [\mathbf{A}_i^i]^H [\mathbf{A}_i^i] (\hat{\mathbf{X}}_i - \mathbf{X}_i) \leq r^2 \quad (3.9)$$

where $\hat{\mathbf{X}}_i$ is the least square solution of $\mathbf{Y}_i = [\mathbf{A}_i^i] \mathbf{X}_i$. After solving the eq. (3.9), we use the result $\tilde{\mathbf{X}}_{i-1}$ and $\tilde{\mathbf{X}}_{i+1}$ to do ICI cancellation by following equation :

$$\tilde{\mathbf{Y}}_i = \mathbf{Y}_i - [\mathbf{A}_{i-1}^i] \mathbf{X}_{i-1} - [\mathbf{A}_{i+1}^i] \mathbf{X}_{i+1}. \quad (3.10)$$

Then using $\tilde{\mathbf{Y}}_i$ to do Sphere Decoding, because the ICI effect comes from \mathbf{X}_{i-1} and \mathbf{X}_{i+1} have been cleaned, we expect that the more correct \mathbf{X}_i can be obtained. Using the procedure as described above iteratively, we expect that the recover performance will be better and better.

Fig 3.2 is the block diagram of the algorithm for one group \mathbf{Y}_i . At initial state, switch links to the path which input a zero vector to do ICI cancellation (i.e. no ICI cancellation). At the $(j+1)$ th iteration, switch links to the path which input $[\mathbf{A}_{i-1}^i](\hat{\mathbf{X}}_{i-1})_j$ and $[\mathbf{A}_{i+1}^i](\hat{\mathbf{X}}_{i+1})_j$ where $(\hat{\mathbf{X}}_{i-1})_j$ represents the output made from the $(i-1)$ th group at the j th iteration for doing ICI cancellation. After ICI cancellation, Sphere Decoding generates $(\hat{\mathbf{X}}_{i-1})_{j+1}$ can be used in ICI

cancellation for next iteration.

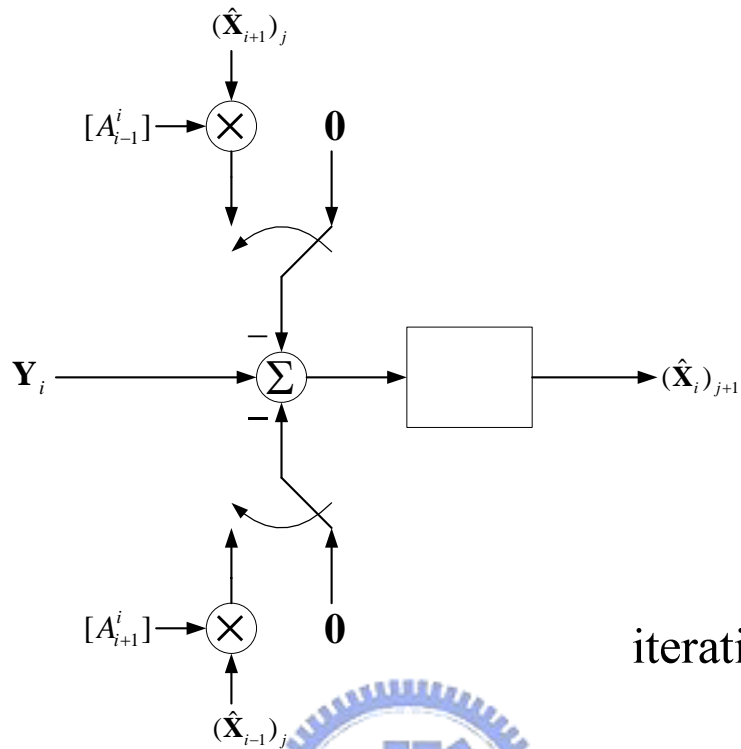


Fig. 3.2 Block diagram of group based ICI cancellation method with Sphere Decoding.

3.3 Group based ICI Cancellation Method with List Sphere Decoding

Different from section 3.2, we apply List Sphere Decoding to generate some candidates of \mathbf{X}_i and use these candidates to compute the soft symbols for doing ICI cancellation.

iteration

initial

3.3.1 Soft Symbol

For QPSK modulation, soft symbol can be calculated as follows :

$$\hat{X}_{k,i} = \frac{1}{\sqrt{2}}(\hat{X}_{k,i}^I + j\hat{X}_{k,i}^Q) \quad (3.11)$$

$$\hat{X}_{k,i}^I = P[X_{k,i}^I = +1 | \mathbf{Y}_i] - P[X_{k,i}^I = -1 | \mathbf{Y}_i] \quad (3.12)$$

$$\hat{X}_{k,i}^Q = P[X_{k,i}^Q = +1 | \mathbf{Y}_i] - P[X_{k,i}^Q = -1 | \mathbf{Y}_i] \quad (3.13)$$

where $\hat{X}_{k,i}^I$ is an expectation of bit corresponding to the real part of the k-th symbol in \mathbf{X}_i .

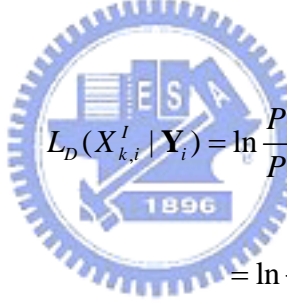
$P[X_{k,i}^Q = +1 | \mathbf{Y}_{i,N_x}]$ is the probability of $\hat{X}_{k,i}^Q$ equals to 1 when c is given and can be

obtained by follows equation :

$$P[X_{k,i}^I = +1 | \mathbf{Y}_i] = \frac{e^{L_D(X_{k,i}^I | \mathbf{Y}_i)}}{1 + e^{L_D(X_{k,i}^I | \mathbf{Y}_i)}} \quad (3.14)$$

$$P[X_{k,i}^I = -1 | \mathbf{Y}_i] = \frac{1}{1 + e^{L_D(X_{k,i}^I | \mathbf{Y}_i)}}$$

where



$$L_D(X_{k,i}^I | \mathbf{Y}_i) = \ln \frac{P[X_{k,i}^I = +1 | \mathbf{Y}_i]}{P[X_{k,i}^I = -1 | \mathbf{Y}_i]} \quad (3.15)$$

$$= \ln \frac{\sum_{\mathbf{X}_i \in L_{k,i,+1}^I} p(\mathbf{X}_i | \mathbf{Y}_i)}{\sum_{\mathbf{X}_i \in L_{k,i,-1}^I} p(\mathbf{X}_i | \mathbf{Y}_i)}$$

and $L_{k,i,+1}^I$ is the set of all possible \mathbf{X}_i that real part of the k-th symbol equal to 1. Here, \mathbf{X}_i

is selected from the list generated by List Sphere Decoding [22]. Assume that the prior

probability of every bit is equal probability and is independent to each other, so we can go

further from eq. (3.15) as follows :

$$L_D(X_k^I | \mathbf{Y}_{i,N_x}) = \ln \frac{\frac{1}{p(\mathbf{Y}_i)} \sum_{\mathbf{X}_i \in L_{k,i,+1}^I} p(\mathbf{Y}_i | \mathbf{X}_i) p(X_{k,i}^I = 1) p(X_{0,i}^I, X_{0,i}^Q, \dots, X_{k,i}^Q, \dots, X_{N_x-1,i}^I, X_{N_x-1,i}^Q)}{\frac{1}{p(\mathbf{Y}_i)} \sum_{\mathbf{X}_i \in L_{k,i,-1}^I} p(\mathbf{Y}_i | \mathbf{X}_i) p(X_{k,i}^I = -1) p(X_{0,i}^I, X_{0,i}^Q, \dots, X_{k,i}^Q, \dots, X_{N_x-1,i}^I, X_{N_x-1,i}^Q)}$$

$$= \ln \frac{\sum_{\mathbf{X}_i \in \mathcal{L}_{k,i+1}^I} p(\mathbf{Y}_i | \mathbf{X}_i)}{\sum_{\mathbf{X}_i \in \mathcal{L}_{k,i-1}^I} p(\mathbf{Y}_i | \mathbf{X}_i)} \quad (3.16)$$

3.3.2 Conditional Probability

From above derivations, if we want to compute the soft symbol then we need to find

$p(\mathbf{Y}_i | \mathbf{X}_i)$. For every subcarrier Y_i , we can use equation below to represent

$$\begin{aligned} Y_i &= a_{ii}X_i + \underbrace{\sum_{\substack{j=1 \\ j \neq i}}^N a_{ij}X_j}_{ICI} + W_i \\ &= \sum_{j \in J_i} a_{ij}X_j + \sum_{j \notin J_i} a_{ij}X_j + W_i \\ \Rightarrow Y_i - \sum_{j \in J_i} a_{ij}X_j &= \sum_{j \notin J_i} a_{ij}X_j + W_i \\ &= n_{I_i} + jn_{Q_i} \\ &= n_i \end{aligned}$$

assume n_{I_i} and n_{Q_i} are independent Gaussian random variable [4], so we need compute the

mean and variance of n_i in order to get $P(Y_i | \mathbf{X}_i)$

$$E[n_i] = E\left[\sum_{j \notin J_i} a_{ij}X_j + W_i\right] = 0 \Rightarrow E[n_{I_i}] = E[n_{Q_i}] = 0 \quad (3.17)$$

$$\sigma_i^2 = \text{Var}[n_i] = E\left[\left|\sum_{j \notin J_i} a_{ij}X_j + W_i\right|^2\right] \quad (3.18)$$

because X_j and W_i are independent, eq. (3.18) becomes

$$\text{Var}[n_i] = P_{av} \sum_{j \notin J_i} |a_{ij}|^2 + \sigma_w^2 \Rightarrow \text{Var}[n_{I_i}] = \text{Var}[n_{Q_i}] = \frac{1}{2} \sigma_i^2. \quad (3.19)$$

The probability $P(Y_i | \mathbf{X}_i)$ can be represented as follows :

$$\begin{aligned}
P(Y_i | \mathbf{X}_i) &= \frac{1}{(\pi\sigma_i^2)^{\frac{1}{2}}} \exp\left[-\frac{n_i^2}{\sigma_i^2}\right] \cdot \frac{1}{(\pi\sigma_i^2)^{\frac{1}{2}}} \exp\left[-\frac{n_Q^2}{\sigma_i^2}\right] \\
&= \frac{1}{(\pi\sigma_i^2)} \exp\left[-\frac{n_i^2 + n_Q^2}{\sigma_i^2}\right] \\
&= \frac{1}{(\pi\sigma_i^2)} \exp\left[-\frac{\|n^2\|}{\sigma_i^2}\right] \\
&= \frac{1}{(\pi\sigma_i^2)} \exp\left[-\frac{\left\|Y_i - \sum_{j \in J_i} a_{ij} X_j\right\|^2}{\sigma_i^2}\right]. \tag{3.20}
\end{aligned}$$

At last, because every n_j in \mathbf{Y}_i can be seen as independent (the correlation of term $\sum_{l \in J_i} a_{jl} X_l$ between each of n_j is small under the assumption that ICI effect comes from neighboring subcarrier.), we can get $p(\mathbf{Y}_i | \mathbf{X}_i)$ as follows :

$$P(\mathbf{Y}_i | \mathbf{X}_i) = \frac{1}{(\pi \det(\Sigma_i))^{N_x}} \exp\left[-(\mathbf{Y}_i - [A_i^i] \mathbf{X}_i)^H \Sigma_i^{-1} (\mathbf{Y}_i - [A_i^i] \mathbf{X}_i)\right] \tag{3.21}$$

where $\Sigma_i = \text{diag}(\sigma_i^2, \dots, \sigma_{i+N_x-1}^2)$.

Above is the case of initial state which ICI cancellation has not been done yet. There are some changes to be done after ICI cancellation. Fortunately, we only need to change the mean and variance of n_j . Again, let's see the subcarrier Y_i after ICI cancellation,

$$\begin{aligned}
\tilde{Y}_i &= Y_i - \sum_{j \in J_i} a_{ij} \hat{X}_j + W_i \\
&= \sum_{j \in J_i} a_{ij} X_j + \sum_{j \in J_i} a_{ij} (X_j - \hat{X}_j) + W_i \\
\Rightarrow \tilde{n}_i &= \tilde{Y}_i - \sum_{j \in J_i} a_{ij} X_j = \sum_{j \in J_i} a_{ij} (X_j - \hat{X}_j) + W_i. \tag{3.22}
\end{aligned}$$

By eq. (3.22), we can derive the mean and variance of \tilde{n}_i as follows :

$$E[\tilde{n}_i] = E\left[\sum_{j \in J_i} a_{ij}(X_j - \hat{X}_j) + W_i\right] = -\sum_{j \in J} a_{ij} \hat{X}_j \quad (3.23)$$

$$\begin{aligned} \text{Var}[\tilde{n}_i] &= E\left[\left|\sum_{j \in J_i} a_{ij}(X_j - \hat{X}_j) + W_i - E[\tilde{n}_i]\right|^2\right] = E\left[\left|\sum_{j \in J_i} a_{ij}X_j + W_i\right|^2\right] \\ &= \sigma_n^2 + P_{av} \sum_{j \in J_i} |a_{ij}|^2. \end{aligned} \quad (3.24)$$

Apply eq. (3.23) and eq. (3.24) into eq. (3.21) then we can get $p(\mathbf{Y}_i | \mathbf{X}_i)$ to compute the soft symbol after ICI cancellation.

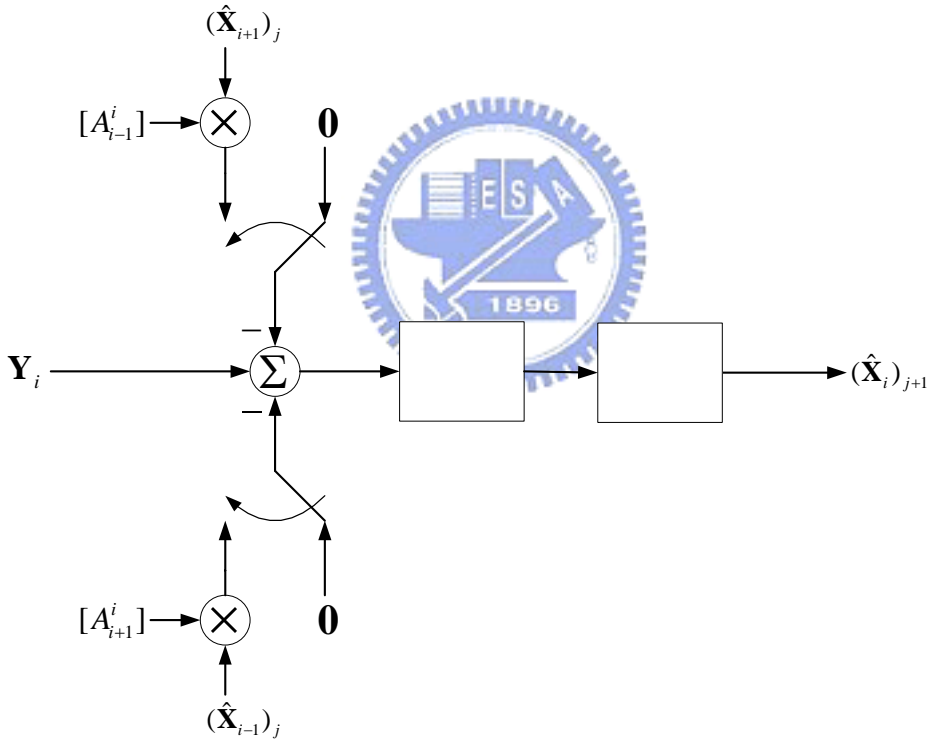


Fig. 3.3 Block diagram of group based ICI cancellation with List Sphere Decoding

The block diagram of the group based ICI cancellation with List Sphere Decoding is showed in fig. 3.3. The procedure is as the same as the one with Sphere Decoding except that Sphere Decoding in fig. 3.2 is replaced by List Sphere Decoding with a soft decision device

followed to compute the soft symbol for ICI cancellation here.

3.4 Radius of the Sphere

In chapter 2, there are two key questions of Sphere Decoding are mentioned. The second one can be solved by the algorithm of Sphere Decoding, but the first one how to choose the radius does not have exactly solution. Here, we use a simple method to decide the initial radius for each application of Sphere Decoding in our group based ICI cancellation method. From eq. (2.21), we use least square solution to be the center of the sphere. We know that least square solution is the best solution to satisfy the ML criterion, but it may not be the feasible solution that is, it may not be a point on the signal constellation. Because of the channel effect, the hard decision of the least square solution may not be the best solution within the all feasible solutions. We can use Fig 3.4 to interpret the problem above. In Fig 3.4, left hand side is the feasible point in transmitted signal space and right hand side is the transformation of left hand side by the channel matrix. On the left hand side, square is the least square solution and the circle is the hard decision of the least square solution. On the right hand side, square \hat{Y}_i is the transformation of the least square solution and circle is the transformation of the hard decision value. Hard decision of the least square is the nearest point of the least square solution within the all feasible points (on the left hand side), but after

transform hard decision is not the nearest point of least square solution's transformation.

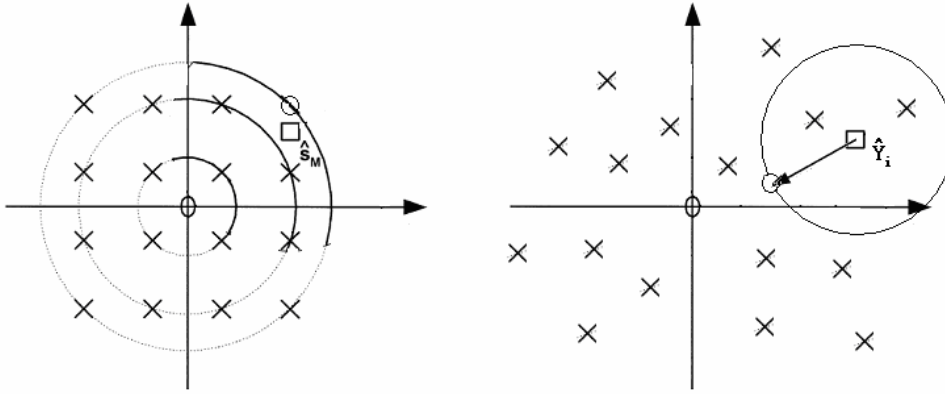


Fig. 3.4 signal space in transmitter and receiver.

If hard decision of least square solution after transformation is not the nearest feasible to the center of the sphere $\hat{\mathbf{Y}}_i$ in the received signal space then the solution which satisfies eq. (2.21) must be inside of the sphere with radius which is equal to the distance between $\hat{\mathbf{Y}}_i$ and the hard decision of least square solution after transformation. By the notion above, it is reasonable to set the initial radius of the sphere to be the distance between $\hat{\mathbf{Y}}_i$ and the hard decision of least square solution after transformation.

Chapter 4

Simulation Result

4.1 Simulation Environment

Simulation results are given for the proposed group based ICI cancellation with Sphere Decoding and List Sphere Decoding under two kinds of simulation environments.

For the first one, a 6 taps channel is considered, and each tap of the channel are modeled as independently complex Gaussian random process which is generated by the Jakes' Doppler spectrum with 120, 240 or 300 km/hr relative velocity. The relative delay of the first tap is zero and others are uniformly distributed in the interval $[0, N_G]$ where N_G is the length of cyclic prefix we used. The power of the path 2, 3, 4, 5 and 6 is 1dB, 9dB, 10dB, 15dB and 20dB smaller than the first path. An OFDM system with $N=256$ subcarriers and quarter phase shift keying (QPSK) are simulated. The carrier frequency is 2.5GHz and the bandwidth of the system is 5MHz. According to the relative velocity and parameter above, $f_d T_s$ equal to 0.0142, 0.0284 and 0.0356. The detail of the parameters can be checked in Table 4.1.

For the second one, a 6 taps channel which is as the same as the first one is considered, but the relatively velocity of the Jakes' Doppler spectrum changes to be 85, 170 or 340 km/hr.

An OFDM system with N=64 subcarriers and quarter phase shift keying (QPSK) are simulated. The carrier frequency is 2GHz and the bandwidth of the system is 200 kHz.

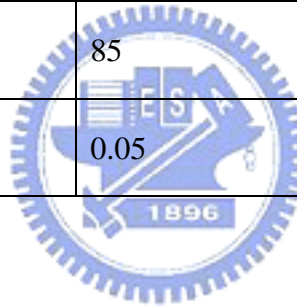
According to the relative velocity and parameter above, $f_d T_s$ equal to 0.05 、0.1 、0.2. The detail of the parameters can be checked in Table 4.2.

Table 4.1 Simulation parameters of the first kind of simulation environment

Modulation	QPSK		
Path	6		
Relative power (dB)	0,-1,-9,-10,-15,-20		
Cyclic prefix length	16		
Carrier frequency	2.5 GHz		
Subcarriers	256		
Bandwidth	5MHz		
Vehicle speed (km/hr)	120	240	300
$f_d T_s$	0.0142	0.0284	0.0356

Table 4.2 Simulation parameters of the second kind of simulation environment

Modulation	QPSK		
Path	6		
Relative power (dB)	0,-1,-9,-10,-15,-20		
Cyclic prefix length	16		
Carrier frequency	2GHz		
Subcarriers	64		
Bandwidth	200kHz		
Vehicle speed (km/hr)	85	170	340
$f_d T_s$	0.05	0.1	0.2



4.2 Simulation Result Discussions

4.2.1 Simulation in Environment I

Fig. 4.1 shows the bit error rate of the OFDM system which applies group based ICI cancellation method with Sphere Decoding, and group size is equal to 8 and Speed is equal to 120 km/hr. The first curve we use group based method without ICI cancellation. We can see that error floor appear when SNR is high if ICI cancellation is not used, and the curve of iteration number equal to 1 and 4 is almost the same as the perfect one which use the correct data of one neighboring groups on each side to do ICI cancellation.

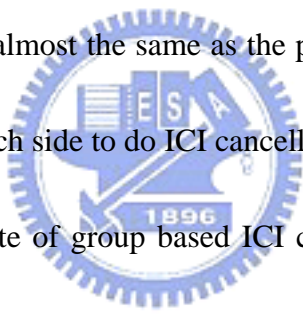


Fig. 4.2 shows the bit error rate of group based ICI cancellation method with Sphere Decoding in different speed with iteration number equals to 4. For high speed case, we can get the diversity gain from ICI but error floor occurs when SNR is high. The performance difference between perfect ICI cancellation and not perfect ICI cancellation is getting larger and larger when speed is getting faster and faster.

Fig. 4.3 shows the bit error rate of group based ICI cancellation method with Sphere Decoding in different group size and speed with iteration number equals to 4. We can see that a larger size of group implies a better performance, but the error floor problem is still not improved by using a larger group size.

Fig. 4.4 shows the difference of bit error rate between group based ICI cancellation method with Sphere Decoding and List Sphere Decoding. LSD can get better performance than SD, but the improvement is not good enough. No matter LSD or SD is applied, the performance still has a gap between perfect one. At last, it seems that group based ICI cancellation method with LSD need less iteration number than SD to get the same performance.

Fig. 4.5 shows the bit error rate of the group based ICI cancellation method with LSD in different group size and speed. Just like the SD case, the performance improvement is not very well for using larger group size. Back to the Fig. 4.3 which use SD, the curve with speed equal to 300km/hr has worse BER than the one with speed equal to 120km/hr at high SNR, but it is different in LSD case the curve with speed equal to 300km/hr still has better BER than the one with speed equal to 120km/hr at high SNR.

Fig. 4.6 and Fig. 4.7 shows the comparison of BER in different group sizes with SD and LSD when the speed is 240 km/hr. Both of SD and LSD, the performances become worse and worse when group size gets smaller and smaller.

Fig. 4.8 and Fig. 4.9 are the comparison between group size equal to 2 and 4 in different speed with SD and LSD. From these two figures, we can find that the performance of group size equals to 2 and 4 are almost the same when speed is equal to 120 km/hr, but the performance of group size equals to 4 is better than equals to 2 when speed equals to 240

km/hr and 300 km/hr. The phenomenon above shows that if ICI effect becomes severer, then we need a larger group.



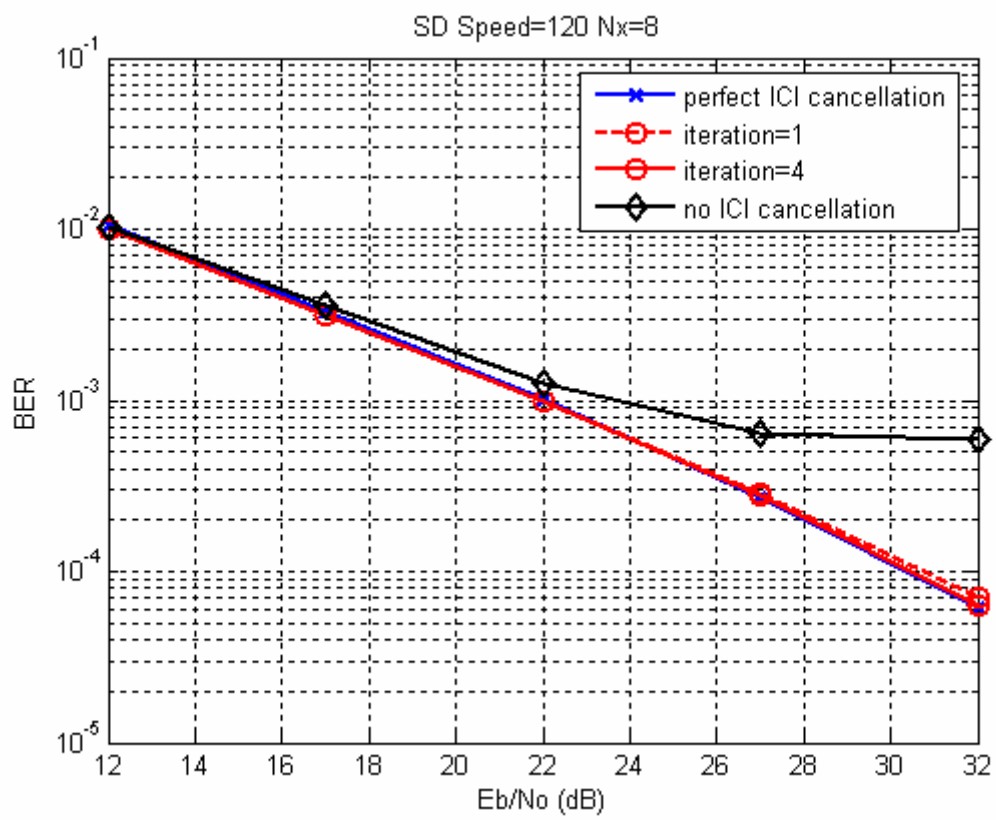


Fig. 4.1 Comparison of BER in different iteration number (I).

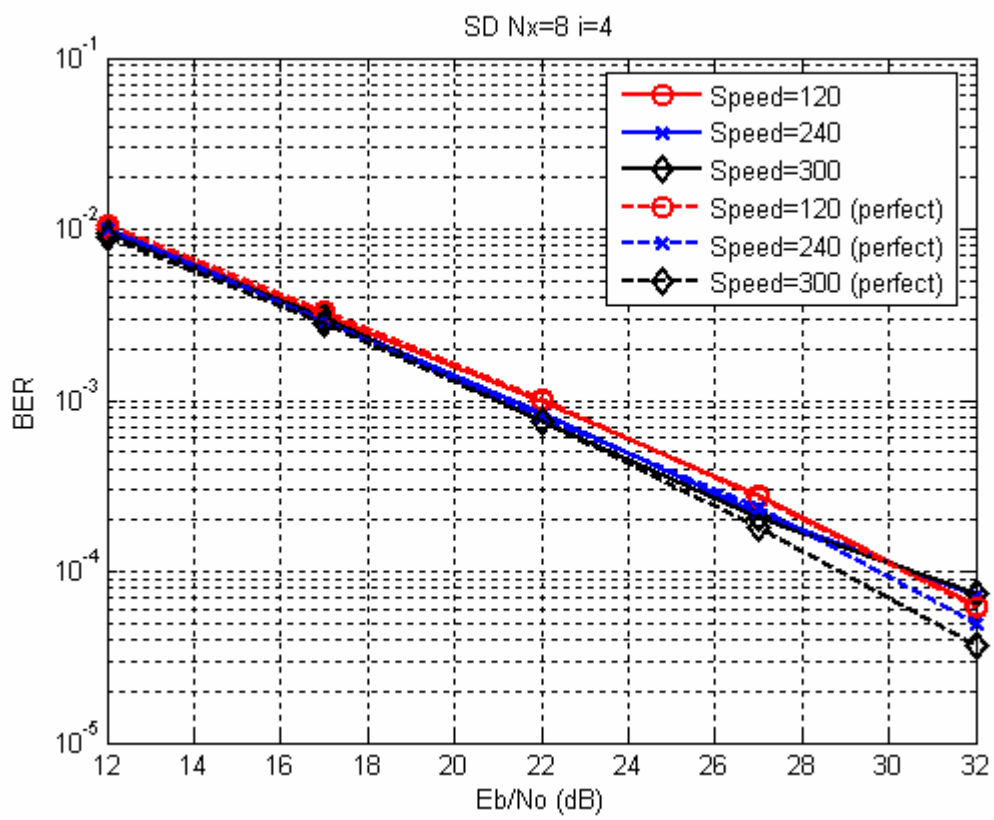


Fig. 4.2 Comparison of BER in different speed (I).

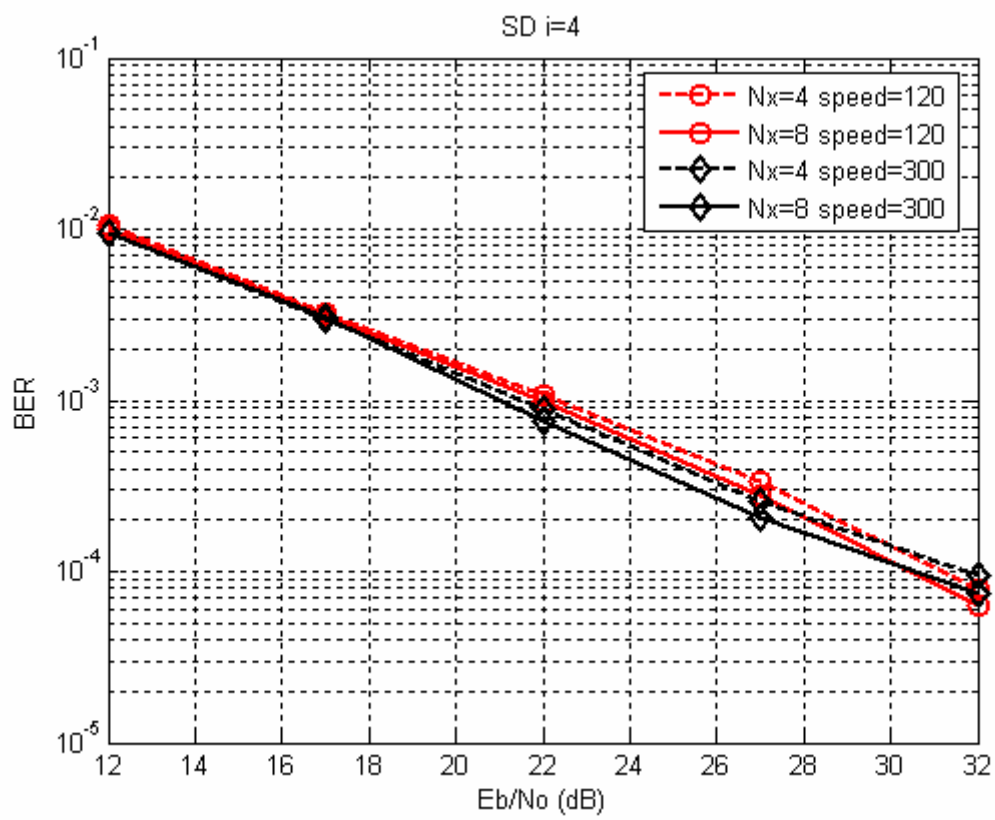


Fig. 4.3 Comparison of BER in different group size (I).

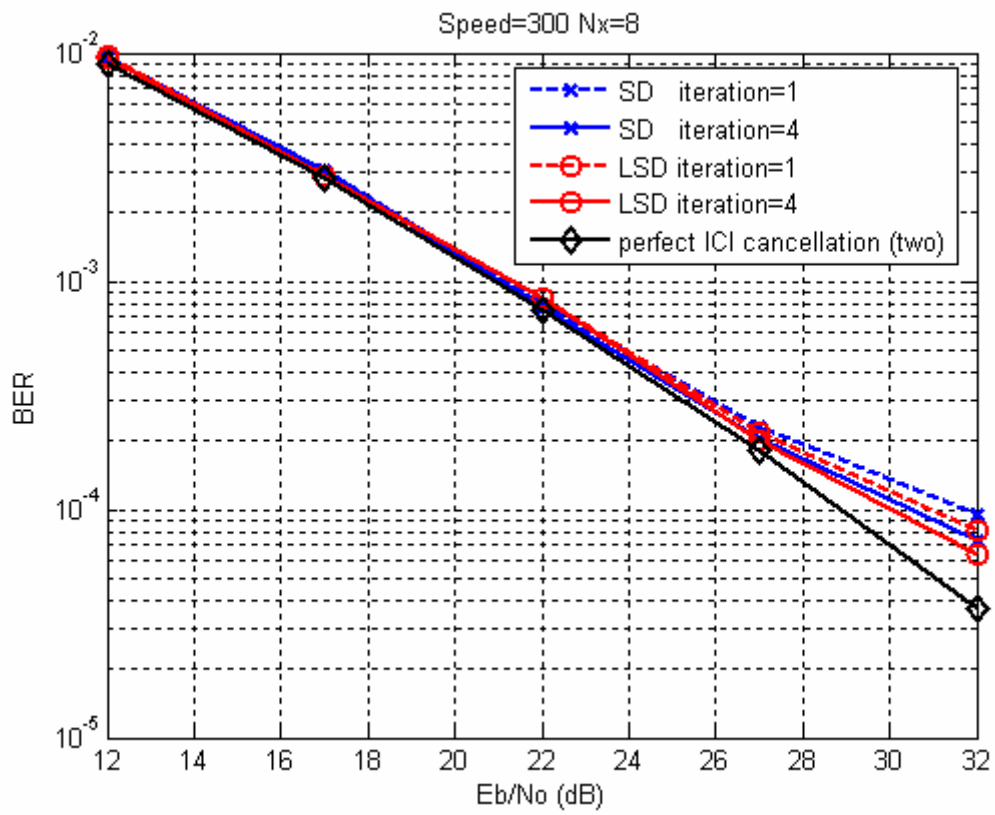


Fig. 4.4 Comparison of BER in different method (I).

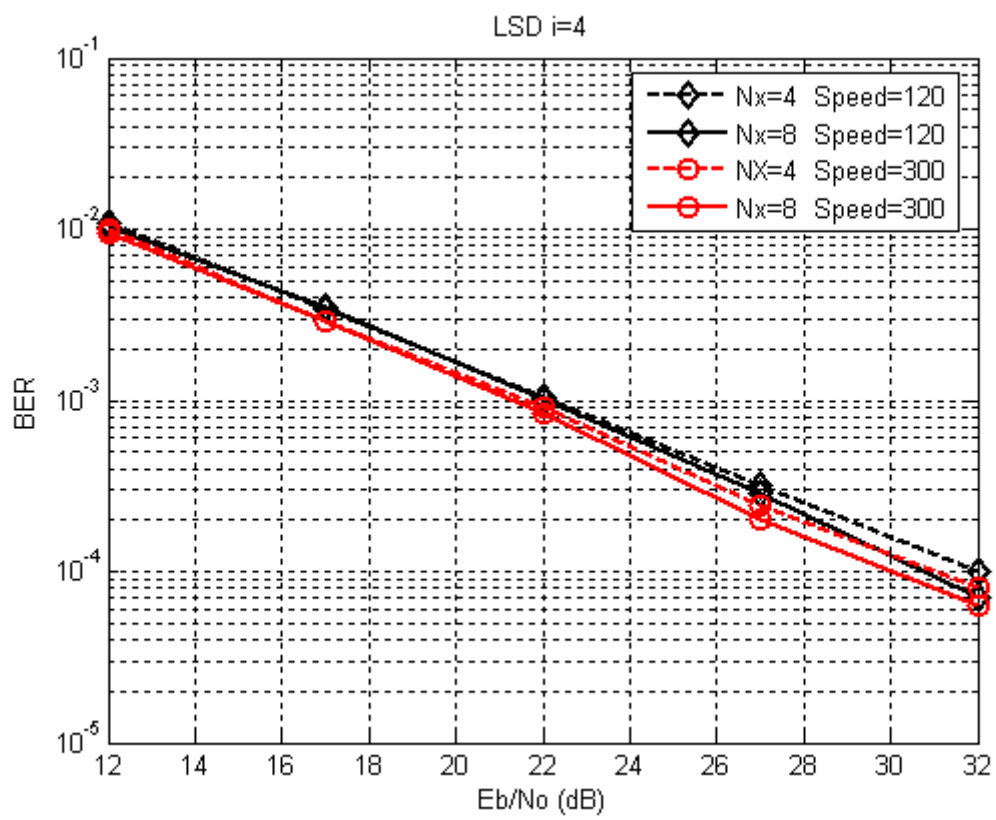


Fig. 4.5 Comparison of BER in different speed and group size (I).

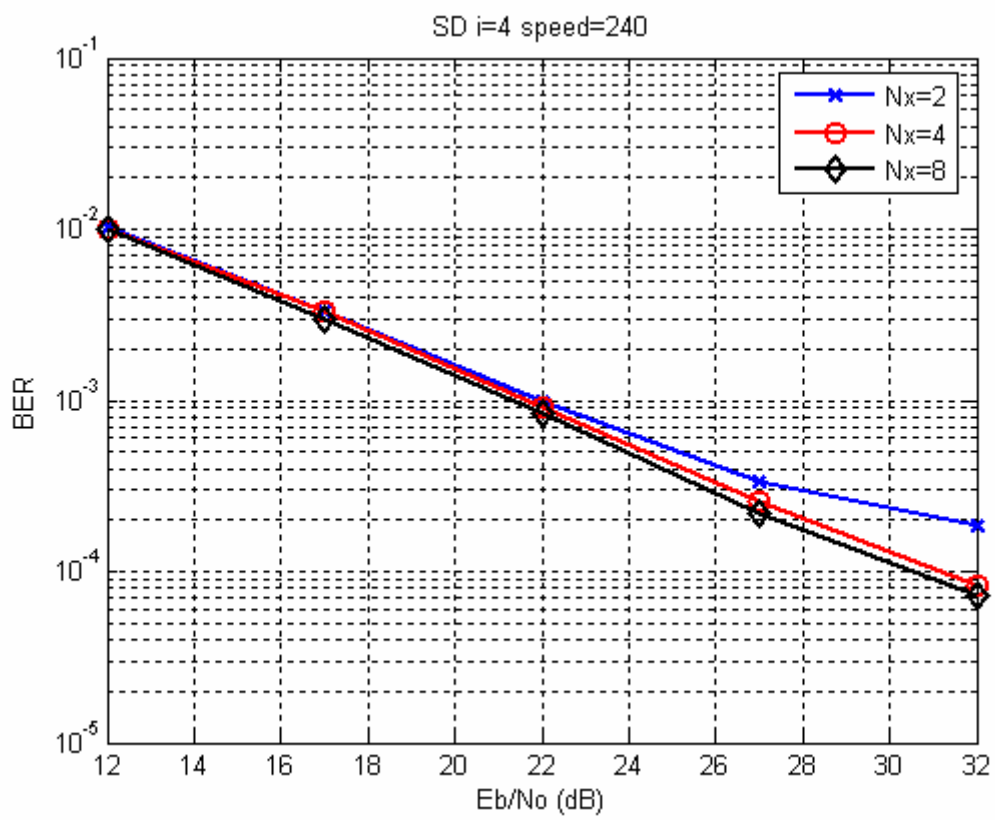


Fig. 4.6 Comparison of BER in different group sizes with SD (I).

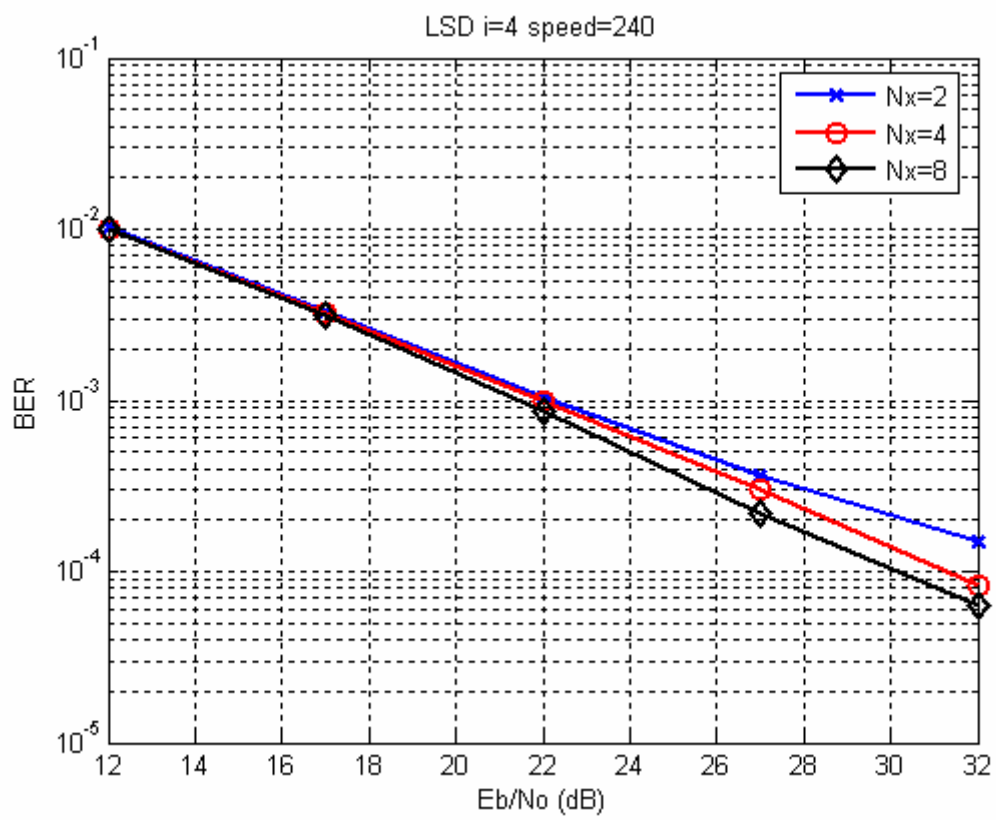


Fig 4.7 Comparison of BER in different group sizes with LSD.

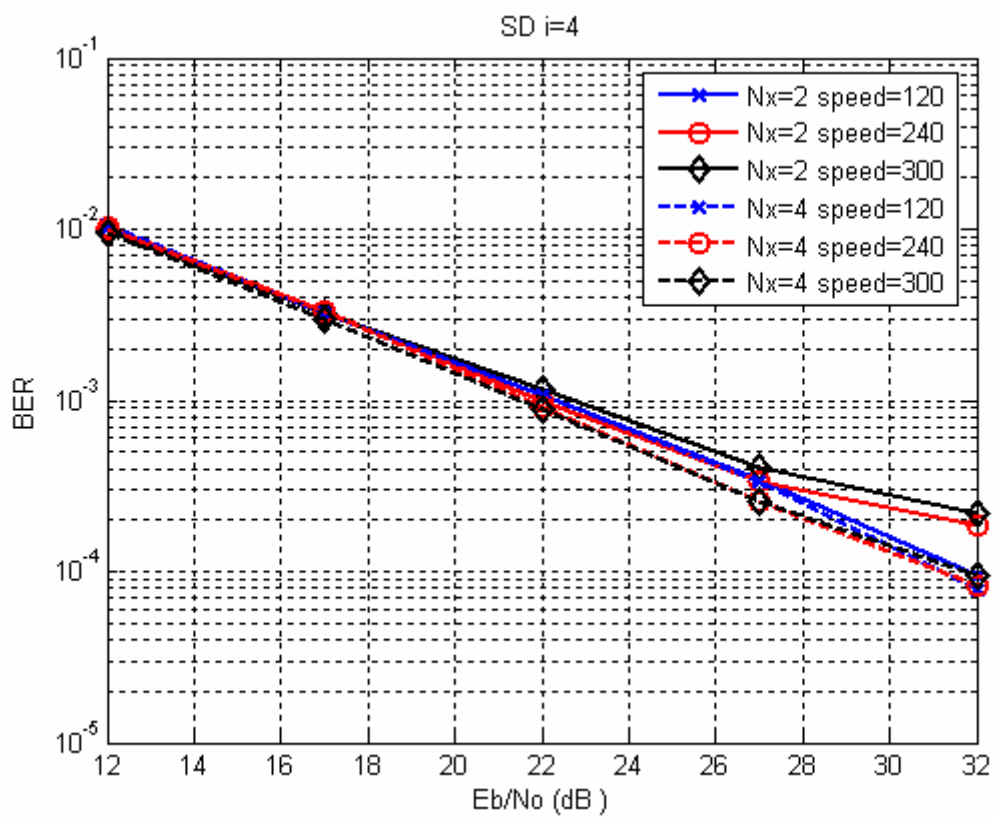


Fig. 4.8 Comparison of BER in different speed and group sizes with SD (I).

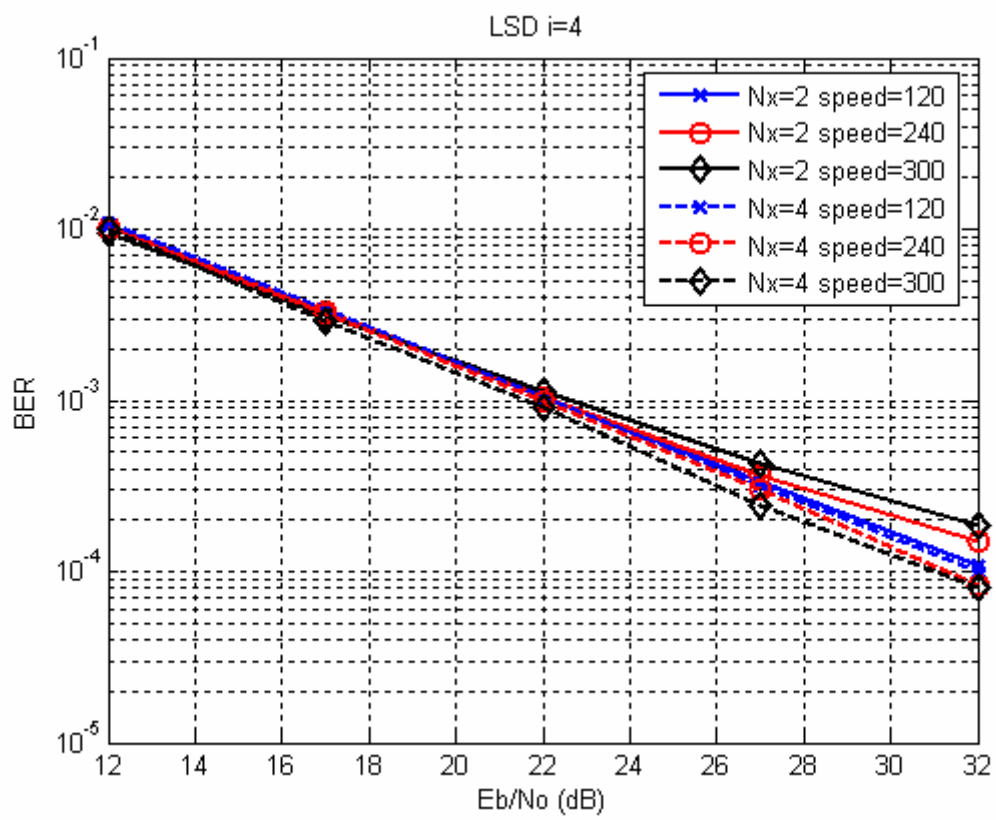
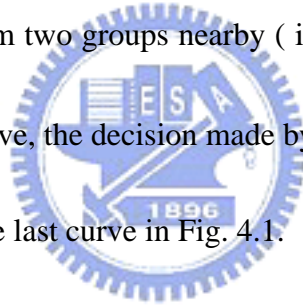


Fig. 4.9 Comparison of BER in different speed and group sizes with LSD (I).

4.2.2 Simulation in Environment II

Fig 4.10 is bits error rate of the group based ICI cancellation method with Sphere Decoding. The sizes of every groups is 8 and we set the window length of ICI is 9. The first line only use group based method without ICI cancellation. We can see that performance gets a lot of improvement by using ICI cancellation. Performance goes better and better with numbers of iteration increasing. Unfortunately, the performance saturates at numbers of iteration equal to 3 and the this performance still much worse than the one (the last curve in Fig. 4.1) which ICI effect comes from two groups nearby (i.e. \mathbf{X}_{i-1} and \mathbf{X}_{i+1} for \mathbf{X}_i) are perfect canceled. By the mention above, the decision made by each groups is not good enough to make the performance closes to the last curve in Fig. 4.1.



In Fig. 4.11, we try different sizes of group. We use 4, 8, 16 three kinds of size and the corresponding ICI windows length are 5, 9 and 17. With numbers of iterations equal to 4, the larger size of group has better performance and higher diversity gain. However, as mention in Fig. 4.1 the error floor still exist because of the accuracy of others group decision.

In Fig. 4.12, we try different kinds of $f_d T_s$. As we know the higher $f_d T_s$ causes severer ICI effect and Fig. 4.3 show the same result. The performance can be improved by using larger size of group, but the improvement still not good enough when $f_d T_s$ is equal to 2 or higher. We also can find that it seems no error floor when $f_d T_s$ equal to 0.05 and size of

group equal to 16. One more thing to be mentioned is that the method we proposed here can get diversity gain from higher $f_d T_s$ in low E_b / N_0 . Compare with the method in [6] which use all the subcarriers to do Sphere Decoding. In the case of $f_d T_s$ equals to 0.1, although we have error floor effect, our method has better performance before E_b / N_0 reaches to 32dB. However, in the case of $f_d T_s$ equals to 0.2, our method has better performance before E_b / N_0 reaches to 22dB.

In Fig. 4.13, we show the performance comparison of group based ICI cancellation method with SD and LSD. As the same as the case of Fig. 4.1, the size of the group is equal to 8 and $f_d T_s$ is equal to 0.1. The solid line represents the method with LSD and dash line represents the method with SD. Different marks represent different numbers of iteration. We can find that the performance of the method with LSD is better the one with SD in every kind of numbers of iteration. We can see that the performance of the method with LSD whose number of iteration is equal to 2 is better than the method with SD whose number of iteration is equal to 3, so the method with LSD has faster speed of being saturation than the method with SD.

In Fig. 4.14, we show that the error floor effect comes from the accuracy of the decision made by groups nearby (we use them to do ICI cancellation) not comes from others group which we do not consider the ICI effect comes from them. The group's size of the solid curve in this figure is equal to 8 and 16 for dash curve. The curve with star mark cancels the ICI

effect perfectly comes from the nearby groups and the curve with diamond mark cancels all the ICI perfectly from other groups except itself. We can see that the dash curve with star and diamond are very close, it means that it does not matter how many groups is taken to do ICI cancellation if the size of group is large enough (also see the curves with star mark). Now look back to the dash curve with circle mark which use the decision of the nearby groups to do ICI cancellation. The different between the dash curve with circle mark and star mark is that the decision of nearby groups is correct or not.



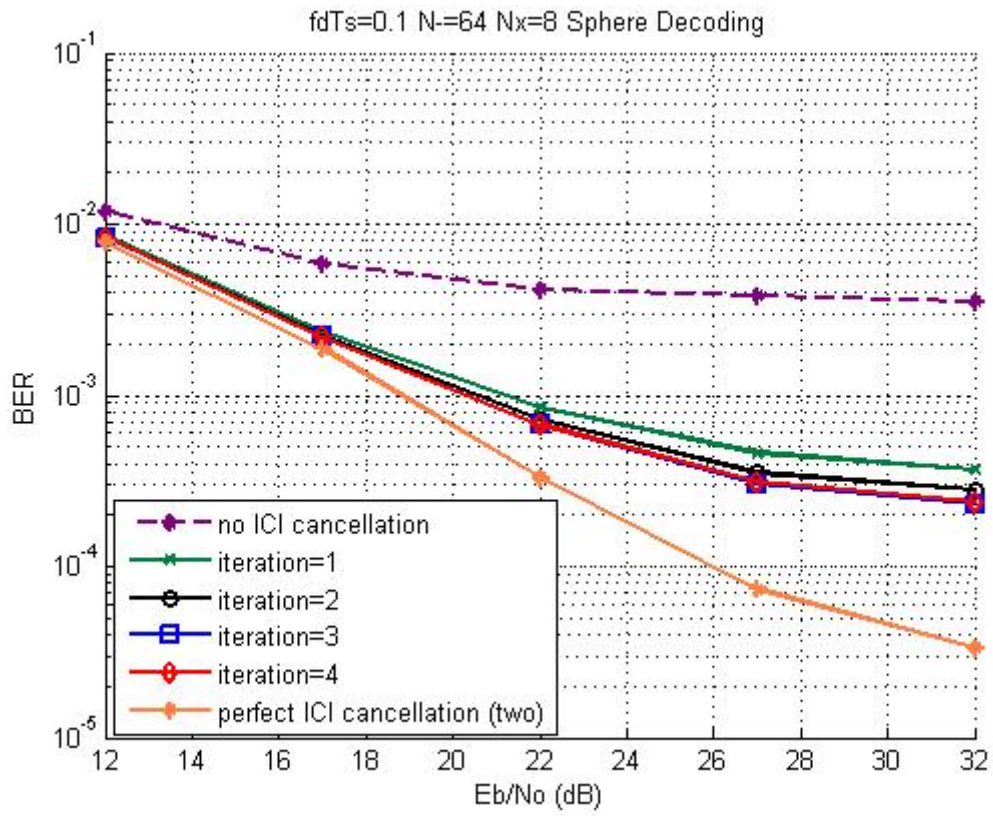


Fig. 4.10 Comparison of BER in different numbers of iteration (II).

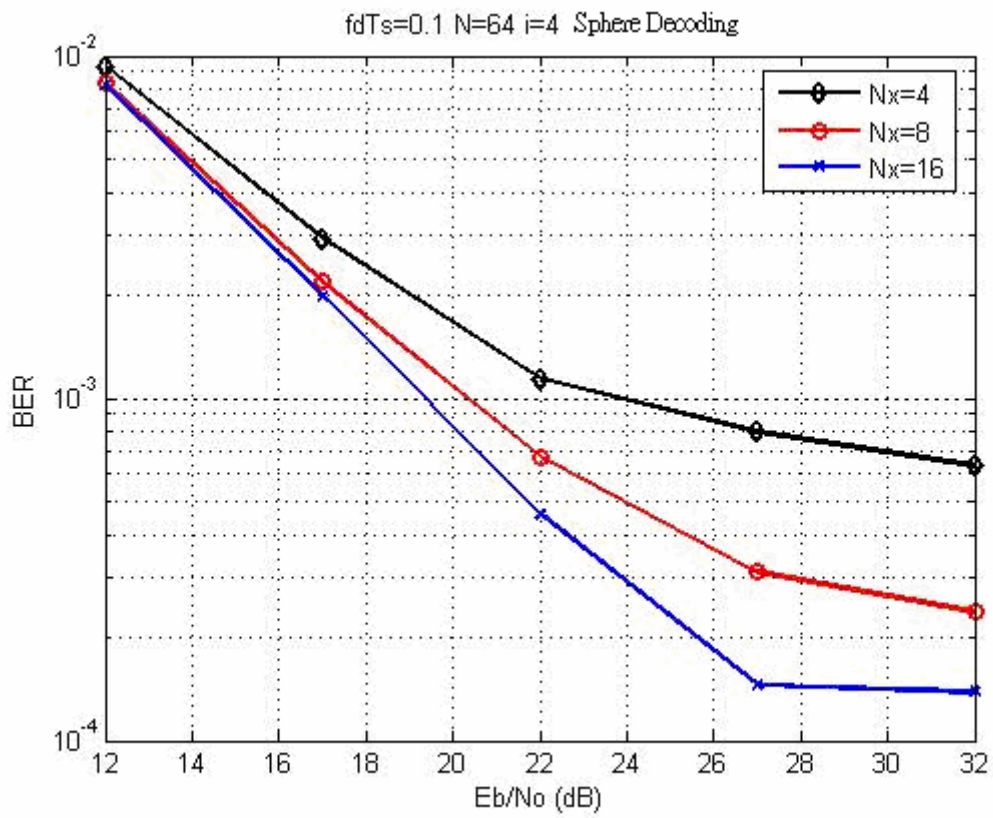


Fig. 4.11 Comparison of BER in different sizes of group (II).

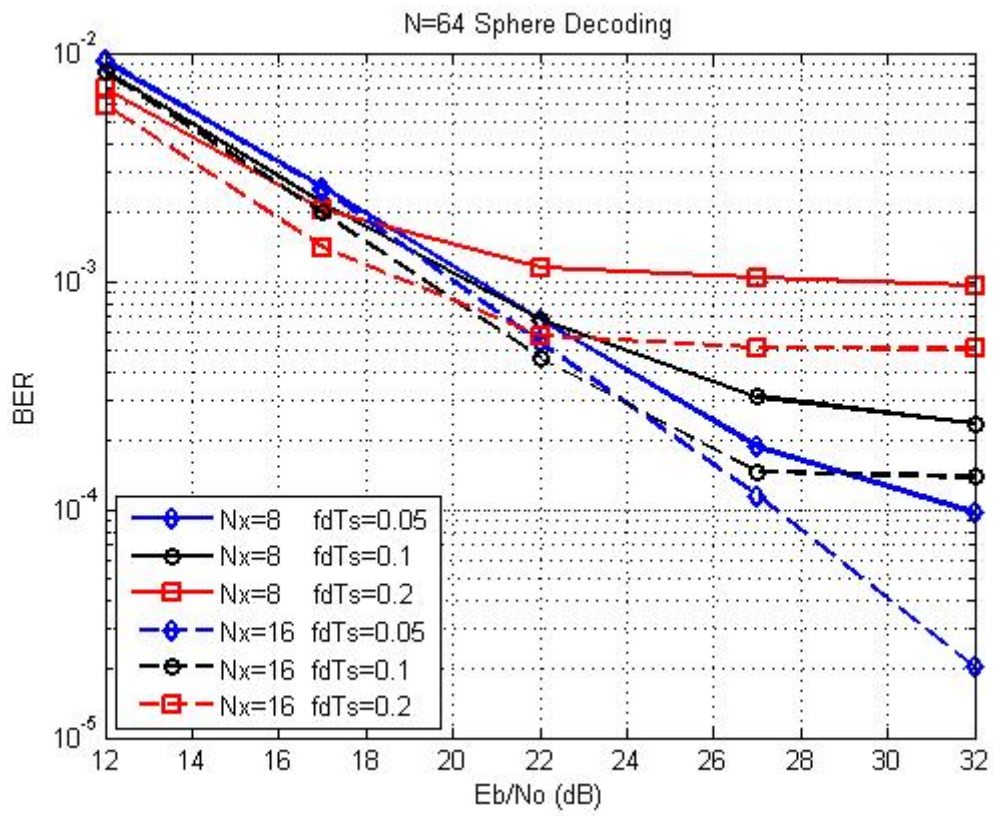


Fig. 4.12 Comparison of BER in different $f_d T_s$ (II).

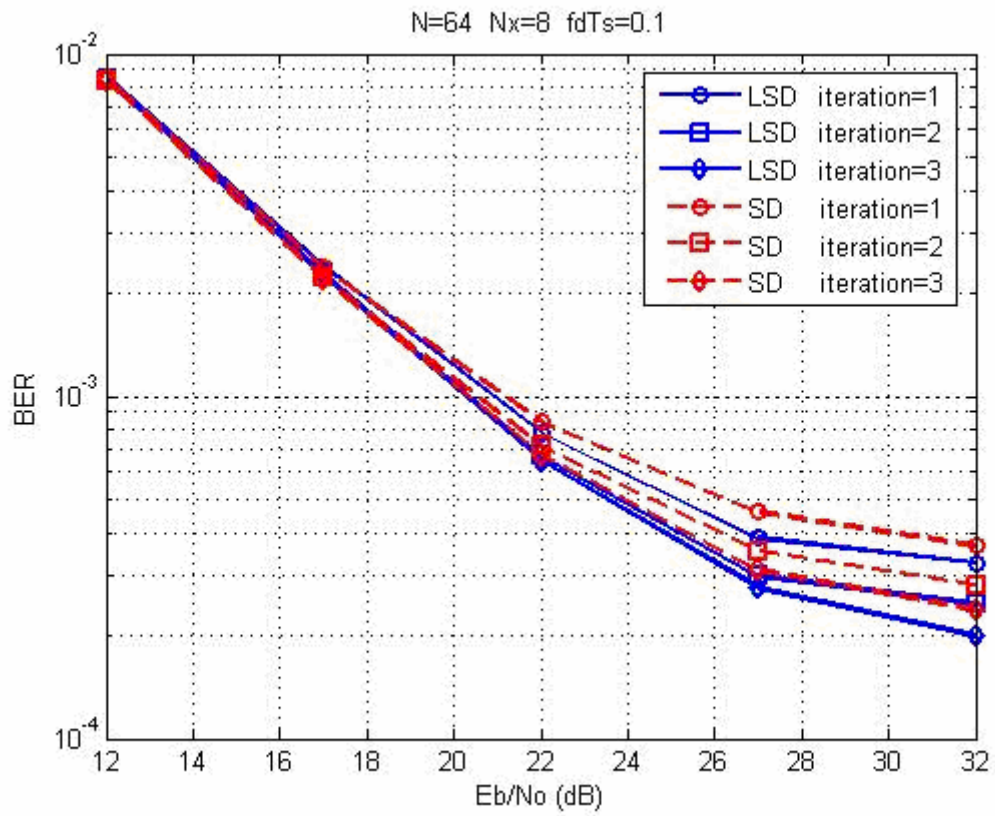


Fig. 4.13 Comparison of BER in LSD and SD (II).

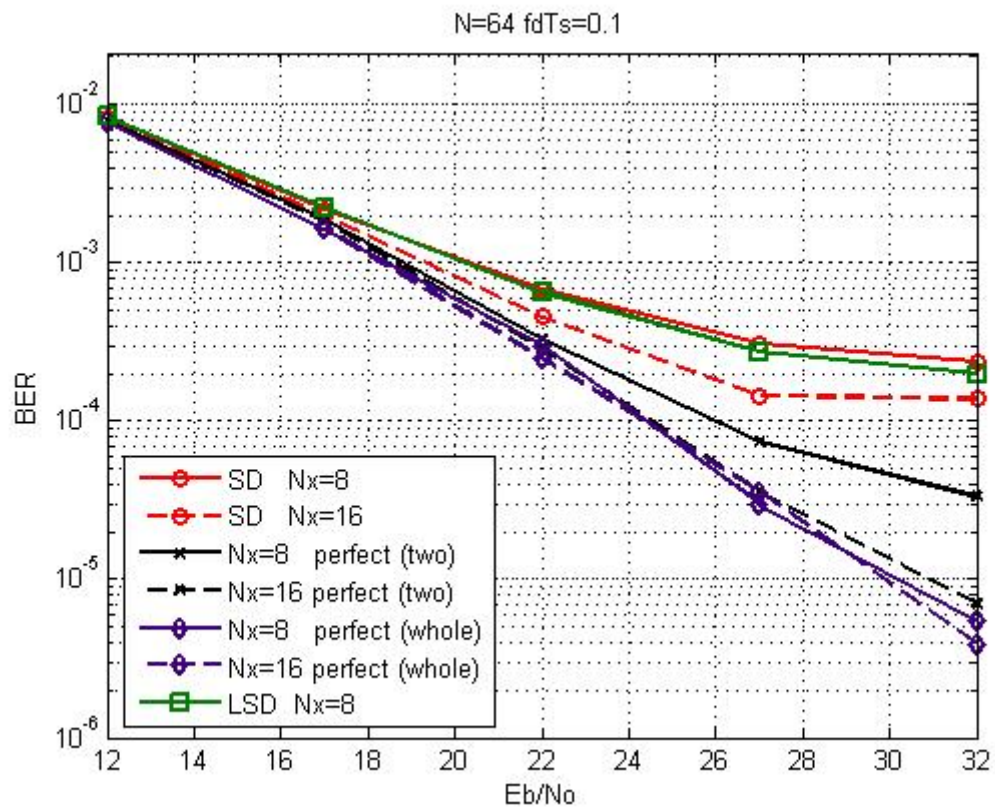


Fig. 4.14 BER performance of group based method with perfect ICI cancellation (II).

4.3 Computational Complexity

The expected complexity of the sphere decoding algorithm is $O(N^3)$ when the signal-to-noise ratio (SNR) is high [23]. Where the sphere decoding algorithm is applied in a subspace of S^N , S is a set corresponding to the modulation scheme and N corresponding to number of subcarriers or group size in group based method. By the notion above, we can get a brief computational complexity comparison (Table 4.3) between the method which using all subcarriers to do Sphere Decoding and the method we propose. Let N denotes number of subcarriers of OFDM system, N_x denotes group size of group based ICI cancellation method, and I denotes the iteration number in group based ICI cancellation method. As we know group based method has N/N_x groups and every group will do Sphere Decoding with N_x subcarriers. The operation of group based method iterative $I+1$ times (include initial state).

In table 4.3 we use an example to make above notion more clearly.

Table 4.4 show the numbers of adder and multiplier are used in group based ICI cancellation method with different sizes of group and general Sphere Decoding without group based method [6] under the second kind of environment which the number of subcarriers N of the OFDM systems is equal to 64. This simulation considers the case which E_b/N_0 is equal to 32dB and for every group based ICI cancellation method the numbers of iteration is equal to 4. The same as we expect, as the group size goes larger and larger the complexity goes

larger and larger. Although, Sphere Decoding without group based method (group size is equal to 64) does not have error floor when E_b / N_0 is high, it is the most complexity one. Comparing group based ICI cancellation with SD and LSD, LSD has more complexity than SD.

Table 4.3 Brief computational complexity comparison

Group based ICI Cancellation method	Sphere Decoding with all subcarriers
$(I + 1)(N / N_x) N_x^3$	N^3
N=256, N _x = 8, I=4	
81920	16777216

Table 4.4 Comparison of computational complexity under the second kind of environment

	SD			LSD
	8	16	64	
Group size	8	16	64	8
Adders	14917	43349	1.6078e8	22465
Multipliers	20426	58554	2.1503e8	29850

Chapter 5

Conclusions

In this thesis, we proposed a group based ICI cancellation method with applying SD and LSD to improve the performance of OFDM in high mobility environment. Because we apply SD or LSD on group based method, the complexity can be reduced a lot. Due to the parallel like ICI cancellation scheme the performance can be improved.

Compare with the group based method which utilizes the serial ICI cancellation [9] , [10]. We can see that there are still a lot of improvements on BER. ICI effect dominates the performance when SNR is high, and it will cause the error floor. Although, the improvement by utilizing the LSD is not very well, it provides a based form for using coding which use soft input and soft output algorithm such as BCJR that exchange the extrinsic information between demapper and decoder [15]. Because we use SD and LSD as tools to solve the ML problem, the complexity can be reduced if the more efficiency SD and LSD is applied even that SD and LSD can be replaced by more powerful method which is used to solve the ML problem or fit this group based structure. At last, in thesis we assume that the channel state information is well known, so the issue combines with channel estimation is needed to be considered.

Bibliography

- [1] Weinstein S. and Ebert P., "Data Transmission by Frequency-Division Multiplexing Using the Discrete Fourier Transform Communications," *IEEE Transactions on [legacy, pre - 1998]*, Volume 19, Issue 5, Part 1, Oct. 1971, Pages(s):628-634.
- [2] William Y.Zou, Yiyang Wu, "COFDM:AN OVERVIEW," *IEEE Transactions on broadcasting*, Volume 41, No.1, Page(s):1-8.
- [3] Y. G. Li and L. J. Cimini, "Bounds on the interchannel interference of OFDM in time-varying impairments," *IEEE Transactions on Communications.*, Volume 49, Mar. 2001, Page(s):401-404.
- [4] Tiejun Wang, John G. Proakis, Elias Masry, and James R. Zeidler, "Performance Degradation of OFDM Systems Due to Doppler Spreading," *IEEE Transactions on Wireless Communications*, Volume 5, No. 6, Jun. 2006, Page(s):1422-1432.
- [5] A. Seyedi and G. J. Saulnier, "General ICI Self-cancellation Scheme for OFDM systems," *IEEE Transactions on Vehicular Technology*, Volume 54, No.1, Jan. 2005, Page(s):198-210.
- [6] Y. J. Kou, W. -S. Lu, and A. Antoniou, "Application of Sphere Decoding in Intercarrier-Interference Reduction for OFDM Systems," *Conference on IEEE PACRIM Communications, Computers and Signal Processing*, Aug. 2005, Page(s):360-363.
- [7] Y. -S. Choi, P. J. Voltz, and F.A. Cassara, "On Channel Estimation and Detection for Multicarrier Signals in Fast and Selective Rayleigh Fading Channels," *IEEE Transactions on Communications*, Volume 49, Aug. 2001, Page(s):1375-1387.
- [8] Xiaodong Cai and Georgios B. Giannakis, "Bounding Performance and Suppressing Intercarrier Interference in Wireless Mobile OFDM," *IEEE Transactions on*

Communications, Volume 51, No. 12, Dec. 2003, Page(s):2047-2056.

- [9] Kwanghoon Kim and Hyuncheol Park, "A Low Complexity ICI Cancellation Methods for High Mobility OFDM Systems," *Proc. IEEE, VTC*, 06Spring, Page(s):2525-2532.
- [10] Hongmei Wang, Xiang Chen, Shidong Zhou, and Yan Yao, "A Low-Complexity ICI Cancellation Scheme in Frequency Domain for OFDM in Time-varying Multipath Channels," *Proc. IEEE PIMRC*, 2005, Page(s):1234-1237.
- [11] J. G. Proakis, "Digital Communications," McGraw-Hill, Boston, 4ed 2001.
- [12] Theodore S. Rappaport, "Wireless Communications, principles and practice," Prentice Hall, 2ed. 1996.
- [13] Alan V. Oppenheim, Ronald W. Schafer and Hohn R. Buck, "Discrete-Time Signal Processing," 2ed 1998.
- [14] Yasamin Mostofi and Donald C. Cox, "ICI Mitigation for Pilot-Aided OFDM Mobile Systems," *IEEE Transactions on Wireless Communications*, Volume 4, No.2, Mar. 2005, Page(s):765-774.
- [15] M. Russell and G. Stuber, "Interchannel Interference Analysis of OFDM in a Mobile Environment," *Proc. IEEE VTC*, Fall 1999, Page(s):329-333.
- [16] Babak Hassibi and Haris Vikalo, "On the Sphere Decoding Algorithm I. Expected Complexity." *IEEE Transactions on Signal Processing*, Volume 53, No.8, Aug. 2005, Page(s):2806-2818.
- [17] Bertrand M. Hochwald and Stephan ten Brink, "Achieving Near_Capacity on a Multiple-Antenna Channel," *IEEE Transactions on Communications*, Volume 51, No.3, Mar. 2003, Page(s):389-399.
- [18] Tao Cui and Chintha Tellambura, "Joint Channel Estimation and Data Detection for OFDM Systems via Sphere Decoding," *GLOBECOM 2004 IEEE*, Page(s):3656-3660.
- [19] Ricardo Santiago Mozos and M. Julia Fernandez-Getino Grrcia, "Efficient Complex Sphere Decoding for MC-CDMA Systems," *IEEE Transactions on Wireless*

Communications, Volume 5, No. 11, Nov. 2006, Page(s):2992-2996.

- [20] Tao Cui and Chintha Tellambura, "An Efficient Generalized Sphere Decoder for Rank-Deficient MIMO Systems," *IEEE Communications Letters*, Volume 9, No.5 May 2005, Page(s):423-425.
- [21] Shaoping Chen and Tianren Yao, "Intercarrier Interference Suppression and Channel Estimation for OFDM Systems in Time-varying Frequency-selective Fading Channel," *IEEE Transactions on Consumer Electronics*, Volume 50, Issue 2, May 2004, Page(s):429-435.
- [22] Yi Hong and Jinho Choi, "A New Approach to Iterative Decoding on coded MIMO Channels," *Proc. IEEE VTC*, Spring 2005, Page(s):1676-1680.
- [23] Jun Tang, Ahmed H. Tewfik and Keshab K. Parhi, "Reduced Complexity Sphere Decoding and Application to Interfering IEEE 802.15.3a Piconets," *Conference on International Communications 2004 IEEE*, Volume 5, Jun 2004, Page(s):2864-2868.

